The Astrophysical Journal, 671:878–893, 2007 December 10

MASS DISTRIBUTION AND PLANET FORMATION IN THE SOLAR NEBULA

S. J. Desch
School of Earth and Space Exploration, Arizona State University, Tempe, AZ 85287-1404; steve.desch@asu.edu
Received 2007 May 4; accepted 2007 August 20

ABSTRACT

The surface density profile $\Sigma(r)$ of the solar nebula protoplanetary disk is a fundamental input to all models of disk processes and evolution. Traditionally it is estimated by spreading out the augmented masses of the planets over the annuli in which the planets orbit today, the so-called minimum-mass solar nebula. Doing so implicitly assumes that the planets completely accreted all planetesimals in their feeding zones, but this assumption has not been tested. Indeed, models of the growth of Uranus and Neptune predict that these planets could *not* have grown to $\sim 10\ M_\oplus$ within the lifetime of the disk, even though they must have, to accrete H/He atmospheres. In this paper we adopt the starting positions of the planets in the "Nice" model of planetary dynamics (Tsiganis and coworkers), in which the solar system started in a much more compact configuration. We derive a surface density profile that is well approximated by the power law $\Sigma(r) = 343(f_p/0.5)^{-1}(r/10\ \mathrm{AU})^{-2.168}\ \mathrm{g\ cm^{-2}}$, where f_p is the fraction of the solid mass in the form of planetesimals. We show that this profile is inconsistent with a steady state accretion disk but is consistent with a steady state decretion disk that is being photoevaporated. We calculate the growth of planets in the context of this disk model and demonstrate for the first time that *all* of the giant planets can achieve their isolation masses and begin to accrete H/He atmospheres within the lifetime of the disk. The fit of our inferred $\Sigma(r)$ to the augmented masses of the planets is excellent (<10%), but only if Uranus and Neptune swtiched places early in the solar system's evolution, a possibility predicted by the Nice model.

Subject headings: Kuiper Belt — Oort Cloud — planetary systems: protoplanetary disks — solar system: formation — stars: formation

1. INTRODUCTION

That the solar system formed from a disklike solar nebula was recognized centuries ago, yet even today our understanding of this process is fundamentally incomplete. Among the most basic unsolved mysteries is the simple fact that Uranus and Neptune each contain at least an Earth mass of hydrogen and helium gas. In order to accrete these light gases, a planet must grow to a mass of about 10 $M_\oplus$ (Mizuno 1980; Pollack et al. 1996), a process that is presumed to take longer than the lifetime of a gaseous disk (typically 3–6 Myr, no more than 10 Myr; Haisch et al. 2001). If we are to understand the formation of these planets, and indeed the structure and evolution of the solar system, models of how matter was distributed in the solar nebula, and how it evolved, are essential.

In response to the great need for an estimate of the distribution of mass in the solar nebula, the "minimum-mass solar nebula" (hereafter MMSN) model was formulated (Edgeworth 1949; Kuiper 1956; Safronov 1967; Alfvén & Arrhenius 1970; Weidenschilling 1977a, hereafter W77; Hayashi 1981; Hayashi et al. 1985). The model of W77 is particularly well developed. In the MMSN model, the metal (i.e., elements heavier than He) contents of the planets are estimated, and solar abundances are used to estimate the original amount of gas (including H and He) associated with each planet. This mass is then assumed to have been distributed in annuli centered on each planet's current locations, and the surface densities are found simply by dividing the "augmented" mass of each planet by the surface area of its annulus. For example, the mass of Jupiter is 318 $M_\oplus$, but it is richer in metals than a solar composition gas. W77 inferred an augmented mass in the range from 600 to $1.2 \times 10^4\ M_\oplus$, distributed in an annulus from 3.3 to 7.4 AU, and so estimated an initial surface density at Jupiter's location (5.2 AU) of about 120–2400 g cm^{-2}. Proceeding in this way for all of the planets, W77 inferred a rough power law for the surface density of gas, Σ, as a function of heliocentric distance r in the solar nebula: $\Sigma(r) \propto r^{-3/2}$, with a large uncertainty in the proportionality constant (and the slope, for that matter). Later, Hayashi (1981) repeated this calculation with differing assumptions about where different solids would condense (especially water ice) and found a minimum value of the proportionality constant consistent with the known planetary masses, deriving a commonly used MMSN surface density:

$$\Sigma(r) \approx 1700\left(\frac{r}{1\ \mathrm{AU}}\right)^{-3/2}\ \mathrm{g\ cm^{-2}}, \qquad (1)$$

with an implied range of validity from inside Mercury's orbit to beyond Neptune's orbit, about 0.3–30 AU.

Integration of the MMSN $\Sigma(r)$ between 0.3 and 30 AU yields a mass of 0.013 $M_\odot$. In comparison, the median mass of protoplanetary disks, derived from millimeter fluxes and assuming a gas-to-dust ratio of 100, is 0.005 $M_\odot$, in both the Taurus star-forming region (Beckwith et al. 1990; Osterloh & Beckwith 1995; Andrews & Williams 2005) and the Orion Nebula cluster (Eisner & Carpenter 2006). It is to be remembered that these inferred masses are subject to large systematic uncertainties to do with the millimeter opacity of dust grains. In addition, it is clear that if only half of the mass of solids is in grains smaller than millimeter sized, then the median masses would have to be doubled. Finally, in both regions, a wide range of disks masses is found, and 1%–2% of disks have masses >0.1 $M_\odot$ (Beckwith et al. 1990; Osterloh & Beckwith 1995; Andrews & Williams 2005; Eisner & Carpenter 2006). With all of these caveats in mind, the MMSN model seems a reasonable approximation to the mass of a typical protoplanetary disk.

Despite its widespread use, it is clear that the MMSN model suffers from many limitations. First, the model assumes that planets accreted all of the solids in their vicinity. It is clear that some fraction f_p of the solids was distributed in planetesimals,

bodies large enough to be captured by planets; the remaining fraction was in the form of dust that was lost as the solar nebula cleared. To the extent that f_p can be estimated, the lost mass can be accounted for by multiplying the inferred mass by f_p^{-1}. However, this still assumes that *all* of the planetesimals in the disk were accreted by planets. In other words, the MMSN model is valid only if planets accreted all of the planetesimals in their feeding zones, that is, if they achieved their isolation masses. This appears to be true for the giant planets but is probably not true for the terrestrial planets. The final stages of planet growth in the terrestrial planet region (0.4–4 AU, roughly) are characterized by a large collection of planetary embryos. Numerical simulations show that during this final stage of assembly, substantial amounts of mass (>50%) are lost and redistributed (e.g., Raymond et al. 2005). It is also quite clear that the asteroid belt and the Mercury region have been severely depleted of solids (W77) at some stage. The underlying assumptions on which the MMSN model is based are probably valid only in the giant planet region, and not in the terrestrial planet region.

A second limitation of the MMSN model is that it is necessarily only a snapshot of the surface density of the protoplanetary disk. Clearly the disk evolved, and a single surface density profile fails to capture this behavior. This becomes especially important when the *growth* of planets, and not just their final masses, is considered. The MMSN model may tell us how much mass (actually, how much solid mass) was available in Uranus's feeding zone, but it does not tell us how long that mass (especially the gas) persisted. And without knowing how long the material persisted, it is difficult to test the underlying assumption that each planet achieved its isolation mass.

Validation of the very concept of using the masses of the planets to infer the surface density of the solar nebula therefore depends on solving three tightly interwoven problems. First, $\Sigma(r)$ must be inferred by *assuming* that the planets reached their isolation masses and so represent the total mass of the disk (at least, all the planetesimals). This $\Sigma(r)$ necessarily represents a snapshot in time of the disk. Second, on the basis of this snapshot, the evolution of the disk over time must be inferred, so that physical conditions in the disk can be calculated as planets grow. Third, the growth of planets must be modeled, to see if they did indeed achieve their isolation masses. These are the ambitious goals of this paper.

The time is right to reexamine the MMSN model because of recent developments in solar system dynamics. The traditional MMSN model (e.g., W77) assumes that the feeding zones of the planets are centered at the present locations. Since the time the MMSN model was published, however, a recognition has grown that the giant planets have all undergone substantial migration to end up where they are found today. Fernandez & Ip (1984) demonstrated that the scattering of leftover planetesimals should have caused Jupiter to migrate inward and the other giant planets to migrate outward. Likewise, the orbit of Pluto is currently understood only in the context of significant outward migration of Neptune (Malhotra 1993). More recently, a new model for the initial structure of the solar system has been advanced, the "Nice" model (Tsiganis et al. 2005; Gomes et al. 2005; Morbidelli et al. 2005). This model successfully explains many diverse observed characteristics of the solar system (discussed in § 2.1) by positing that the giant planets formed between 5 and 15 AU rather than from 5 to 30 AU. If true, this means that the MMSN model must be updated substantially, as the same mass of planets would have been concentrated in about $\frac{1}{4}$ the area previously thought, raising the typical surface density by a factor of 4 over that of W77. The variation of $\Sigma(r)$ with r would also be steeper; in fact, in this paper we infer $\Sigma(r) \propto r^{-2.168}$. The consequences of such a steep profile on models of disk evolution are profound.

This paper is organized as follows. In § 2 we update the MMSN model to account for the starting positions of the planets predicted from the Nice model, as well as other constraints. We infer a surface density for the solar nebula, which is well approximated by $\Sigma(r) = 343(f_p/0.5)^{-1}(r/10\ \mathrm{AU})^{-2.168}$ g cm^{-2}, which is much denser and steeper than the traditional MMSN model. In § 3 we consider disk models that potentially could lead to such a steep surface density profile. By necessity we restrict our attention to so-called α viscosity disk models. We find two such models that potentially could match our inferred $\Sigma(r)$. The first is a commonly considered model, a rapidly evolving, viscously spreading disk. The second model is new and involves a quasi–steady state disk with a photoevaporated outer edge. Both match our inferred $\Sigma(r)$ at at least one instant in time, and neither can be ruled out on this basis. A common feature of these two models is that both are characterized by outward net flow of mass through the outer solar system at the time of planet formation, implying that the solar nebula was a decretion disk. In § 4 we consider the growth of planets within the context of these models. We show that in the viscously evolving disk, the surface density of gas decreases with time too rapidly to assist in the formation of planets, but in the photoevaporated disk, growth of all of the giant planets is possible. In the context of the photoevaporated disk, Uranus and Neptune are able to acquire H and He atmospheres, and the giant planets can be shown to have achieved their isolation masses, validating the assumptions on which the solar nebula is based. In § 5 we summarize our conclusions regarding the structure, evolution, and formation environment of the solar nebula.

2. A NEW MINIMUM-MASS SOLAR NEBULA

To derive the original surface density of the solar nebula from planetary masses, one must estimate the original disk mass associated with each planet, as well as the size and location of each planet's feeding zone. In this section we outline the results of the Nice model, including the starting locations of the giant planets and the mass of the planetesimal disk beyond the giant planets. We then review constraints on the augmented masses of the giant planets. We recalculate the surface density of the MMSN model. We lastly review the chronological constraints that reveal *when* these surface densities apply.

2.1. *The Nice Model*

We first consider the locations at which the planets formed, which are not necessarily the locations where they orbit today. We adopt the starting conditions of the Nice model (Tsiganis et al. 2005; Morbidelli et al. 2005; Gomes et al. 2005; Levison et al. 2007). This model postulates that the giant planets were initially in circular ($e \sim 10^{-3}$), coplanar ($i < 0.1^\circ$) orbits, with Jupiter orbiting at 5.45 AU (slightly farther from the Sun than today), Saturn a few tenths of an AU inside the 2:1 mean motion resonance (MMR) with Jupiter, or 8–9 AU, and Uranus and Neptune at about 11–13 and 13.5–17 AU, respectively. Another feature central to the Nice model is a disk of planetesimals beyond these planets, out to about 30 AU, totalling $\approx 35\ M_\oplus$ in mass. Planetesimals at the inner edge of this disk were scattered by the outermost planet, many of them inward. These planetesimals gravitationally interacted with the planets and caused the inward migration of Jupiter and the outward migration of the other planets. The key to the Nice model is that after several 100 Myr,

Jupiter and Saturn crossed their mutual 2:1 MMR, causing chaotic behavior in the outer solar system for several tens of Myr. Most notably, Uranus and Neptune rapidly migrated outward chaotically, probably scattering off of each other; in 50% of their simulations, Tsiganis et al. (2005) observed the two planets to switch places. This so naturally explains why Neptune's mass exceeds that of Uranus that we henceforth assume that such an exchange took place and that the original order of the planets was Jupiter, Saturn, Neptune, Uranus (we return to this point below). Following this chaotic orbital evolution, the rapid outward migration of Neptune through the planetesimal disk rapidly depleted it. A small fraction of the mass, $\sim 10^{-3}$ (or 0.04 $M_\oplus$), was scattered outward to become the modern-day scattered Kuiper Belt. Planetesimals are also scattered inward (and the inward migration of Jupiter scatters asteroids), causing the late heavy bombardment (LHB). The trapping of Jovian Trojans is explained quantitatively by this model. Finally, as Neptune ran out of material to scatter, its outward migration is halted at about 30 AU. The outward migration of Neptune explains the existence of two dynamical classes of Kuiper Belt objects, or KBOs (a dynamically cold population with inclinations $<4^\circ$ and a dynamically excited population with inclinations as high as 30°), and it explains the large number of KBOs trapped in Neptune's MMRs. The Nice model does not especially constrain the mass of planetesimals far beyond 30 AU, and the observed abrupt decrease in the number of classical (low eccentricity) KBOs with semimajor axes >47 AU (Chiang & Brown 1999; Trujillo & Brown 2001) is not an immediate prediction of the Nice model (Morbidelli et al. 2007). The Nice model does very successfully explain, quantitatively, the final semimajor axes, eccentricities, and inclinations of the giant planets. The Nice model explains so many aspects of solar system architecture that we adopt it fully here and consider the consequences of the starting conditions of this model.

The Nice model places many important constraints on the solar nebula. In order for the final eccentricities and inclinations of the giant planets to resemble those of the present-day solar system, Jupiter must start at about 5.45 AU, and Saturn somewhere around 8–8.5 AU. There is better agreement in these quantities, as well as in the semimajor axis of Uranus, if one of the ice giants has an encounter with one of the gas giants; this in turn implies that Saturn and Neptune started <3.5 AU apart in semimajor axis. Uranus and Neptune probably formed at least 2 AU apart, but a compact system is favored. Gomes et al. (2005) were able to match the configuration of the giant planets today and simultaneously include the constraints from the LHB, by assuming that the planets started at heliocentric distances as follows: Jupiter, 5.45 AU; Saturn, 8.18 AU; Neptune, 11.5 AU; and Uranus, 14.2 AU. This implies that the planets each have feeding zones about 3 AU wide (roughly 10 Hill radii). The total mass of the planetesimal disk beyond Uranus is constrained to be about 35 $M_\oplus$. This mass is needed to match the mass of the Jovian Trojans and the mass of the Kuiper Belt; more importantly, for masses >40 $M_\oplus$, the final separation of Jupiter and Saturn is too large. We therefore adopt 35 ± 5 $M_\oplus$ for this part of the disk. This mass resided in an annulus from about 16 AU (just outside Uranus's feeding zone) to about 30 AU (where Neptune stopped its outward migration).

An additional constraint comes from the timing of the LHB, which must occur about 650 Myr after the formation of the solar system (Tera et al. 1974). As found by Gomes et al. (2005), the time taken for Jupiter and Saturn to reach their 2:1 MMR and trigger the LHB is sensitive to the separation Δa between the planetesimal disk inner edge and the orbit of the outermost planet, increasing as some power of Δa. Specifically, Gomes et al. (2005) find that the delay is 600 Myr if $\Delta a = 1.0$ AU and ≈900 Myr if $\Delta a = 1.3$ AU. For $\Delta a > 1$ AU, these data suggest that the delay is (very roughly) $\approx 650(\Delta a/1\ \mathrm{AU})$ Myr. These timescales were obtained utilizing a single surface density of planetesimals at the inner edge of the planetesimal disk, $\Sigma_{\mathrm{inner}} = 0.52$ g cm^{-2}, corresponding to a surface density of gas $\Sigma = 70(f_p/0.5)^{-1}$ g cm^{-2} at the inner edge, where f_p is the fraction of the mass of condensable solids that is in planetesimals. These numbers arise from the starting condition in Gomes et al. (2005), 1.9 $M_\oplus$ of planetesimals per 1 AU annulus, which implies a surface density falling off as r^{-1}. If the surface density fell off with distance faster than r^{-1}, then for the same amount of mass the surface density at the inner edge would be greater (and at 30 AU would be smaller). A higher surface density Σ_{inner} would decrease the time taken for Jupiter and Saturn to reach their mutual 2:1 resonance, presumably as $\Sigma_{\mathrm{inner}}^{-1}$. We estimate the inner edge of the planetesimal disk to lie about 1.7 AU past the location where Uranus formed, so that Uranus would form at the geometric mean of the radii of the inner and outer edges of its feeding zone [$(12.8 \times 15.9)^{1/2} \approx 14.2$]. Given the time delay arising from $\Delta a = 1.7$ AU, we estimate that the timing constraint of the LHB can still be satisfied if Σ at the inner edge is 1.7 times that implicitly assumed by Gomes et al. (2005), or $\approx 120(f_p/0.5)^{-1}$ g cm^{-2} at 15.9 AU. Because the timing of the LHB depends on a degenerate combination of Δa and Σ_{inner}, neither quantity is particularly well constrained. Conversely, this means that many values of Σ_{inner} are potentially consistent with the timing of the LHB and the 2:1 resonance crossing. More to the point, just because Gomes et al. (2005) assumed a distribution of mass in the planetesimal disk $\Sigma(r) \propto r^{-1}$ (thereby fixing Σ_{inner} for $\Delta a = 1.0$ AU) does not mean that other surface density profiles are inconsistent with the timing of the LHB. A profile $\Sigma(r) \propto r^{-2}$ is equally consistent, despite Σ_{inner} being larger, provided that Δa is also larger.

Finally, one last constraint comes from the migration of Neptune. After Jupiter and Saturn crossed their 2:1 MMR and had scattered Neptune out past 15 AU, Neptune continued to scatter planetesimals and migrate outward. The total mass of planetesimals that Neptune scattered on its way to its location at 30.1 AU was 35 ± 5 $M_\oplus$, according to the Nice model (Tsiganis et al. 2005; Gomes et al. 2005). Simulations of Neptune's migration show that it can undergo runaway migration, in which case it migrates until it reaches the edge of the planetesimal disk, or damped migration, in which case its migration stalls because there are too few planetesimals to scatter (Gomes et al. 2004). In runaway migration, Neptune's migration usually stops when the outer edge of the disk of planetesimals is reached, and one explanation for Neptune's final location at 30 AU is that the disk of planetesimals ended there (Morbidelli et al. 2007). During damped migration, Neptune's semimajor axis would continue to increase, but at exponentially smaller rates, asymptoting to a final value. Thus, Neptune's migration could also halt if the surface density of planetesimals got too low; this is the explanation we adopt here. The onset of damped migration and therefore the location where Neptune's migration halts are most sensitive to the local surface density of planetesimals. Gomes et al. (2004) find that this critical value is ~ 1.5 $M_\oplus$ per annulus 1 AU wide, at a distance of 30 AU, which is consistent with a surface density of planetesimals ≈ 0.22 g cm^{-2}. This is consistent with their finding that Neptune's migration can be halted at 30 AU in a disk with 50 $M_\oplus$ between 20 and 50 AU with a $\Sigma \propto r^{-4}$ profile. In such a disk, the surface density would vary from 1.27 g cm^{-2} at the

inner edge to 0.033 g cm^{-2} at the outer edge, but it would equal 0.22 g cm^{-2} at 31 AU. In a disk with $\Sigma \propto r^{-1}$ and 50 $M_\oplus$, this density is reached at 30 AU, by which point Neptune's 2:1 resonance has begun to migrate out of the disk (which ends at 50 AU), accelerating Neptune's migration. In a disk with $\Sigma \propto r^{-1}$ with only 45 $M_\oplus$, this critical surface density is reached at 27 AU, which is where Gomes et al. (2004) observe Neptune to cease its migration (see their Fig. 6). Finally, in a disk with $\Sigma \propto r^{-1}$ with only 40 $M_\oplus$, the critical surface density is reached at 24 AU, which is again where Neptune is observed to cease its migration. We conclude that in a variety of disks, Neptune ceases migration when the surface density of planetesimals reaches 0.22 g cm^{-2}, and that this therefore must have been the initial surface density of planetesimals in the solar nebula disk, at 30.1 AU.

2.2. *Augmented Masses*

We now consider the augmented masses of the planets and the extrapolation to a mass of solar nebula material. If the giant planets accreted gas and solids both, in the proportions characteristic of a solar composition gas, they would be about 1.5% condensable solids (Lodders 2003), the remainder being hydrogen and helium gas. Commonly, these solids are collectively called "metals" and labeled *Z*. (NB: The astronomical definition of *Z* technically includes abundant noble gases like Ne, which here we consider part of the gas; here *Z* should be taken to mean condensable solids, not astronomical metals.) In fact, the metal content, M_Z, of each planet greatly exceeds 1.5%, ranging from about 6% for Jupiter to over 80% for Neptune (see below). This indicates that gas and solids were segregated during the growth of the planets. Solid material locked up in very small ($\approx$1 μm in size) particles—dust—is dynamically very well coupled to the gas, and it is difficult to imagine how dust and gas could be segregated. Solid material locked up in very large ($\approx$1 km in size) particles—planetesimals—is dynamically decoupled from the gas. We therefore distinguish between these two populations. Models of the dynamics and growth of solids in the solar nebula tend to find that particles smaller than centimeters in size are dynamically well coupled to the gas, objects tens of meters in size essentially orbit in Keplerian fashion, and bodies of intermediate size tend to drift significantly with respect to the gas (Weidenschilling 1977b; Weidenschilling & Cuzzi 1993; Cuzzi & Weidenschilling 2006). It is also generally found that objects smaller than tens of meters tend to follow a size distribution that is in collisional equilibrium, with growth by coagulation balancing fragmentation by collisions (Kenyon & Luu 1999; Weidenschilling 2000). For our purposes, we define planetesimals as solid objects greater than about 10 m in radius. We denote as f_p the fraction of the mass of all solids that is locked up in planetesimals. The value of f_p is uncertain, but simulations suggest $f_p \approx 0.5$ (Weidenschilling 2000); that is, about half of the mass of solids in the solar nebula grows to planetesimal sizes.

The fraction of a solar composition gas that can condense into solids is small. From Table 11 of Lodders (2003), these are the percentages of the total mass of a solar composition gas (which is >98% H and He) that can condense as solids: 0.489% into "rock" (silicates, oxides, metal, and FeS), 0.571% into water ice, 0.330% into methane ice, and 0.097% into ammonia ice. In regions of the nebula where all of these species condensed, only a fraction $1/67.2 = 1.5\%$ of the mass can condense into solids; in regions where only rock and water ice condense, the fraction is $1/94.3 = 1.1\%$. Throughout the outer solar nebula, temperatures are presumably <150 K, and water ice and rock should condense fully, but the condensation of C and N is not assured. A reasonable estimate to the temperatures in the regions where the planets formed is given by the formula of Chiang & Goldreich (1997),

$$T(r) = 150\left(\frac{r}{1\ \mathrm{AU}}\right)^{-0.429}\ \mathrm{K}. \quad (2)$$

According to this formula, the temperatures at the locations where Jupiter, Saturn, Neptune, and Uranus started (in the Nice model) are 72, 61, 53, and 48 K, respectively. Nitrogen can condense as ammonia hydrates at 131 K, or as N_2 clathrate at 58 K (Lodders 2003). Whether N was in the form of N_2 or ammonia hydrates, it should have fully condensed at Neptune, Uranus, and in the planetesimal disk beyond. Nitrogen probably condensed fully at Saturn's location as well. The nitrogen in Titan's atmosphere is isotopically heavy, strongly implying that Titan formed with a large reservoir of condensed nitrogen that has largely escaped (Lunine et al. 1999). Likewise, C can condense as refractory organic material, as methane clathrate below 78 K, or as methane ice below 41 K (Lodders 2003). We assume that at Saturn's location and beyond C fully condensed as well. Finally, many heavy elements, including C and N, appear to be similarly enhanced by factors of 2–4 in Jupiter's atmosphere (Niemann et al. 1998). Based on this, we assume that these elements also condensed in Jupiter's formation region.

Because the fraction of solar composition gas that is solids is so small, it is unlikely that the giant planets acquired much of their metal content M_Z from dust. For Jupiter, $M_Z \approx 10$–$42\ M_\oplus$ (Guillot 2005), so the envelope mass is about 300 $M_\oplus$. Based on the solar abundances described above, the metal content acquired from the envelope could not exceed about $4(1 - f_p)\ M_\oplus$, or about 2 $M_\oplus$ if $f_p = 0.5$. Thus, Jupiter acquired 80%–98% of its metal content from accreting planetesimals; for the other planets the proportions are generally higher. It is generally accepted that the giant planets formed by "core accretion," a two-stage process in which first a planetary core of rock and ices grows until it reaches a critical mass capable of accreting gas (and dust) directly from the solar nebula (Mizuno et al. 1978; Mizuno 1980; Bodenheimer & Pollack 1986; Pollack et al. 1996; but for an alternative hypothesis, "disk instability," in which Jupiter gravitationally collapsed from the gas within the solar nebula, see Boss 2000). In the context of the core accretion model, many planetesimals were necessarily accreted during the planetary core stage, although planetesimals could also be accreted later, directly into the planet's gas envelope (and at a rate distinct from the accretion of gas). Regardless of when the solids were acquired, the metal content of a planet is a direct measure of the mass of *planetesimals* in the solar nebula. This is obviously also true of the planetesimal disk beyond the giant planets that is a part of the Nice model. The mass of all *solids* in the solar nebula was necessarily higher by a factor of f_p^{-1}.

Reconstruction of the solar nebula surface density of gas is possible by determining the augmented mass of each planet, the mass of solar nebula gas associated with the metal content of each planet. Based on the above discussion, the augmented mass associated with each planet is

$$M_{\mathrm{aug}} = M_Z f_p^{-1}\left(\frac{\mathrm{gas}}{\mathrm{solids}}\right), \quad (3)$$

where the gas-to-solids ratio is in the range 67.2–94.3. This augmented mass is then divided by the surface area associated with each planet's feeding zone.

We first estimate the metal content of Uranus and Neptune and the planetesimal disk. Where these objects formed, presumably all solids condensed and the gas/solids ratio was 67.2. The disk, with mass $\approx 35 \pm 5\ M_\oplus$, therefore yields an augmented mass $2353 \pm 336\ M_\oplus$ times $2(f_p/0.5)^{-1}$. The masses of Uranus and Neptune are, respectively, 14.9 and 17.2 $M_\oplus$. These objects are mostly rock and ices; assuming that methane and ammonia condensed, the planetary interior models of Podolak et al. (2000) place upper limits on the H/He contents of Uranus and Neptune of 4.2 and 3.2 $M_\oplus$, respectively. If hydrogen and helium are only present in the upper atmosphere, a lower limit of 0.5 $M_\oplus$ is obtained for each planet (Guillot 2005). The expected ranges of M_Z are then 10.7–14.4 $M_\oplus$ for Uranus and 14.0–16.7 $M_\oplus$ for Neptune. These numbers are consistent with the expectation that M_Z is about 30% larger for Neptune than for Uranus, based on the difference in their mean densities (1.27 g cm^{-3} for Uranus vs. 1.64 g cm^{-3} for Neptune). We accordingly assume $M_Z \approx 12.55 \pm 1.55\ M_\oplus$ for Uranus, yielding an augmented mass $843 \pm 124\ M_\oplus$ times $2(f_p/0.5)^{-1}$. For Neptune we assume $M_Z = 15.35 \pm 1.35\ M_\oplus$, yielding an augmented mass $1032 \pm 91\ M_\oplus$ times $2(f_p/0.5)^{-1}$.

Saturn has a mass of 95.2 $M_\oplus$ and a mean density 0.69 g cm^{-3}. Clearly Saturn is mostly gas, but it also possesses a rocky core and a total metal content similar to those of Uranus and Neptune. Models of Saturn's interior are more complex, relying on complicated equations of state to derive the mass of its core and its overall metal content. We use the results of Saumon & Guillot (2004), who show that Saturn's core mass lies in the range 9–22 $M_\oplus$ (i.e., $16 \pm 6\ M_\oplus$); the mass of metals in the envelope is independently constrained to lie in the range 1–8 $M_\oplus$ (i.e., $5 \pm 3\ M_\oplus$). The combined metal content of Saturn is then $M_Z = 21 \pm 7\ M_\oplus$. Assuming again that N and C fully condensed at Saturn, this yields an augmented mass for Saturn of $1411 \pm 470\ M_\oplus$ times $2(f_p/0.5)^{-1}$.

The augmented mass of Jupiter, with total mass 317.8 $M_\oplus$ and mean density 1.33 g cm^{-3}, is even more difficult to infer because it is sensitive to the equation of state at even higher pressures, which is highly uncertain. One constraint comes from the composition of Jupiter's atmosphere, measured by the *Galileo* probe, which shows enrichments of metals above solar composition, by factors of 2–3 (Niemann et al. 1998). The latter fact immediately suggests a mass of metals in the envelope of 9–18 $M_\oplus$ (Guillot 2005). The mass of Jupiter's core theoretically could range from 0 to 20 $M_\oplus$, depending on the high-pressure equation of state assumed (Saumon & Guillot 2004), although smaller core masses $<10\ M_\oplus$ are clearly favored (Guillot 2005). If Jupiter formed by core accretion, it must have started with a core of at least 5–10 $M_\oplus$ (Mizuno 1980; Pollack et al. 1996) to accrete gas. However, vigorous convection within Jupiter subsequently may have eroded this core (Guillot et al. 2004). As the core mass potentially could dominate Jupiter's metal content, M_Z for Jupiter must be considered highly uncertain. Guillot (2005) suggests $M_Z = 10$–$42\ M_\oplus$. This yields an augmented mass for Jupiter of $1747 \pm 1075\ M_\oplus$ times $2(f_p/0.5)^{-1}$, if C and N fully condensed (or a factor of 1.40 times larger if they did not). The range of possible augmented masses for Jupiter is quite large, from $\sim$700 to $\sim$4000 $M_\oplus$ (times f_p^{-1}). These values lie squarely in the range of augmented masses assumed by W77 but are a factor of 3 smaller on the high end.

2.3. *Surface Density of the Solar Nebula*

In Table 1 we compile our assumed starting locations of the planets, their feeding zones, their augmented masses, and our inferred surface density of the solar nebula. Our assumed starting locations of the giant planets are identical to the values favored by Gomes et al. (2005). The inner radius of Jupiter's feeding zone was chosen so that Jupiter lay at the geometric mean of the inner and outer radii of its feeding zone, that is, $r_{\rm in} = r_0^2/r_{\rm out}$. The location of the planetesimal disk beyond Uranus is set equal to the geometric mean of the inner radius of 15.9 AU and the outer radius of 30 AU, which is the maximum distance out to which Neptune managed to scatter planetesimals as it migrated outward.

TABLE 1
Initial Solar System Conditions

Planet	$M_{\rm aug}$[a] ($M_\oplus$)	$r_{\rm in}$ (AU)	r_0 (AU)	$r_{\rm out}$ (AU)	Σ[a] (g cm^{-2})
Jupiter	1747 ± 1075	4.45[b]	5.45	6.68	546.8
Saturn	1411 ± 470	6.68	8.18	9.70	244.5
Neptune	1032 ± 91	9.70	11.5	12.8	123.2
Uranus	843 ± 124	12.8	14.2	15.9[a]	77.2
Disk[c]	2353 ± 336	15.9[b]	22.5	30.0	31.2

[a] Augmented masses and surface densities should be multiplied by a factor $2(f_p/0.5)^{-1}$.
[b] The inner edge of Jupiter's feeding zone and the outer edge of Uranus's feeding zone were chosen so that the planets formed at the geometric mean of the inner and outer radii of their feeding zones.
[c] Refers to the primordial disk of planetesimals beyond Uranus and Neptune.

In Figure 1 we have plotted the surface densities inferred from the giant planets and the planetesimal disk, as well as their locations. We also plot a least-squares linear fit to these five data points; that is, we find a power-law relationship between $\Sigma(r)$ and r.

We find a best-fit line of

$$\Sigma(r) = 343\left(\frac{f_p}{0.5}\right)^{-1}\left(\frac{r}{10\ \mathrm{AU}}\right)^{-2.168}\ \mathrm{g\ cm^{-2}}. \qquad (4)$$

The standard MMSN formula, $\Sigma(r) = 1700(r/1\ \mathrm{AU})^{-1.5}$ g cm^{-2}, or $\Sigma(r) = 54(r/10\ \mathrm{AU})^{-1.5}$ g cm^{-2}, is plotted for comparison. As expected, the surface density is increased by roughly a factor of 4 over the standard formula and falls off more steeply with r, using the more compact starting conditions of the Nice model.

We find it astonishing that the augmented masses of the planets should yield a surface density profile so closely fitted by a single line. Our best guesses for the surface densities match the fit to within 10% for Jupiter and Saturn and to within 1% for Neptune, Uranus, and the planetesimal disk. Our inferred surface density profile conforms to the upper and lower limits imposed by all five objects. The theoretical uncertainties displayed in Figure 1 are not standard deviations, but if we were to treat them as such, we would derive a goodness-of-fit parameter $\chi_\nu^2 = 0.03$. This is to be compared to the surface density derived by W77. Although he fitted a single power law [$(\Sigma(r) \propto r^{-3/2}$] to the profile, this is clearly not justified. A fit through the Jupiter and Saturn region overestimates the mass in the Uranus and Neptune zones; a fit through the Uranus and Neptune zones overestimates the mass in the Jupiter and Saturn zones; and fits through either far overestimate the mass in the Mercury, Mars, and asteroid zones. Indeed, if the starting locations of the planets according to the Nice model (Tsiganis et al. 2005; Gomes et al. 2005) are correct, then such a good correlation could not have been found until 2 years ago.

We also find it remarkable how readily the *additional* constraints from the Nice model (beyond the planet starting locations) fit into the same surface density profile derived from the planetary augmented masses. The mass of the disk of planetesimals

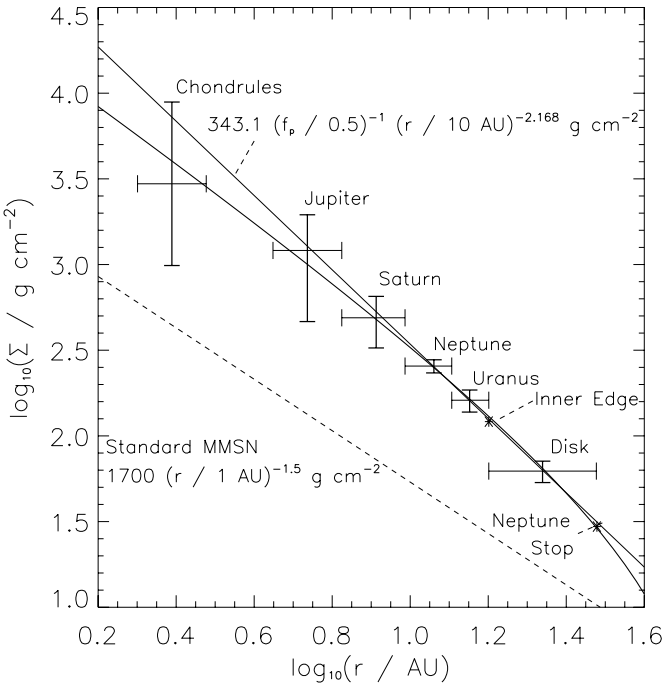

FIG. 1.—Distribution of mass in the solar nebula. Vertical bars reflect the theoretical uncertainties in the augmented masses of the planets. Vertical bars run through the presumed starting location of each planet. Horizontal bars span the assumed feeding zones of each planet and should not be interpreted as uncertainties. Horizontal bars run through the surface density corresponding to the presumed augmented mass of each object. The solid line depicts the least-squares fit using the four giant planets and the planetesimal disk ("Disk") that lay beyond Uranus and Neptune. The derived fit, $343(f_p/0.5)^{-1}(r/10\ \mathrm{AU})^{-2.168}$ g cm^{-2} (graphed here assuming $f_p = 0.5$), differs significantly from the standard MMSN formula (eq. [1]), $\Sigma(r) = 1700(r/1\ \mathrm{AU})^{-1.5}$ g cm^{-2}. It is much larger (even if $f_p = 1$), and it alone is consistent with the surface density of gas in the chondrule-forming region ("Chondrules"). Additional constraints from the timing of the LHB ("Inner Edge") and the location where Neptune stopped migrating ("Neptune Stop") are depicted. The thick line is our fit based on a photoevaporating decretion disk, described in § 3.

scattered by Neptune was inferred from indirect dynamical arguments, yet it exactly conforms to the profile derived from the giant planets. Likewise, assuming that Uranus formed at the geometric mean of its feeding zone so that its feeding zone extended 1.7 AU beyond its formation location, we infer a surface density from the timing of the LHB, at the inner edge of the planetesimal disk, that also conforms to our inferred surface density profile. Assuming that the migration of Neptune transitioned from runaway to damped migration and then halted where the surface density of planetesimals fell below a critical value, the surface density at 30 AU *also* conforms to our inferred surface density profile.

Altogether, seven mass constraints combine to define a single monotonic surface density profile $\Sigma(r)$. This in itself is surprising, but not as surprising as the significance of this trend. The surface density profile we infer is much denser and has a steeper variation with r than the traditional MMSN. The slopes that could simultaneously fit all the planetary masses are limited to a range from -1.79 to -2.53. The shallower slope of the standard MMSN, -1.5, is therefore excluded. We also infer a disk mass between 2 and 30 AU of $\approx 0.060(f_p/0.5)^{-1}\ M_\odot$, about 5 times greater than the mass in the standard MMSN model in the same range of radii. Most shockingly, our fit very strongly implies that Uranus and Neptune switched places when Jupiter and Saturn crossed their 2:1 MMR resonance. Fits to the surface densities of just Jupiter and Saturn, or of Jupiter, Saturn, and the planetesimal disk, yield profiles very similar to the fit in Figure 1. Had we derived the surface density at 11.5 AU using the augmented mass of Uranus and the surface density at 14.2 AU using the augmented mass of Neptune, the surface density at 11.5 AU would be reduced by 0.1 dex and the surface density at 14.2 AU raised by 0.1 dex. These seem like small changes, but they exceed the uncertainties in the augmented masses for these planets and are formally excluded. Again treating the range of augmented masses as standard deviations, fits with Uranus and Neptune in their current positions yield $\chi^2_\nu > 2$, but if their original order had Neptune form at 11.5 AU and Uranus at 14.2 AU, the fit is improved to $\chi^2_\nu = 0.03$. We view this as strong, if circumstantial, evidence that Neptune did indeed form closer to the Sun than Uranus.

Also included in Figure 1 is an estimate of the surface density in the asteroid belt region, 2–3 AU, derived from models of chondrule formation. Desch & Connolly (2002) and Ciesla & Hood (2002) have explained multiple aspects of chondrule formation with a model in which chondrules are melted in large-scale shocks propagating through the solar nebula gas. For reasonable shock speeds ($V_s < 10$ km s^{-1}), the peak temperatures and cooling rates of chondrules are reproduced for gas densities in the chondrule-forming region $\rho \approx (0.3\text{–}3) \times 10^{-9}$ g cm^{-3}. Assuming that the disk is vertically isothermal, hydrostatic equilibrium yields a density profile $\rho(z) = \rho(z = 0) \exp(-z^2/2H^2)$, where $H = C/\Omega$, C being the sound speed and Ω being the Keplerian orbital frequency. Vertically integrating the gas density yields a surface density $\Sigma = (2\pi)^{1/2}\rho(r, 0)H$. Assuming $r = 2.5$ AU and a temperature of 100 K yields $C = 0.6$ km s^{-1}, $\Omega = 5.1 \times 10^{-8}$ s^{-1}, and $H = 1.2 \times 10^{12}$ cm $= 0.080$ AU. If $\rho(r, 0) \approx 1 \times 10^{-9}$ g cm^{-3}, give or take a factor of 3, this implies $\Sigma(r = 2.5\ \mathrm{AU}) = 2960$ g cm^{-2}, give or take the same factor of 3 (and independent of f_p). Even the lowest surface density consistent with chondrule formation in nebula shocks is a factor of about 2.3 times larger than the surface density of 430 g cm^{-2} predicted by the traditional MMSN model for this region. Put another way, combining our assumed temperature profile (eq. [2]) with our derived surface density (eq. [4]) yields a midplane gas density

$$\rho_{\mathrm{gas}}(r, 0) = 1.93 \times 10^{-11} \left(\frac{f_p}{0.5}\right)^{-1} \left(\frac{r}{10\ \mathrm{AU}}\right)^{-3.4537} \mathrm{g\ cm^{-3}}. \quad (5)$$

At 2.5 AU, this yields a midplane gas density 2.3×10^{-9} g cm^{-3} (assuming $f_p = 0.5$), consistent with chondrule formation in nebular shocks. The traditional MMSN model would predict $\rho_{\mathrm{gas}} \approx 1.5 \times 10^{-10}$ g cm^{-3} in the same region, too low to lead to chondrule formation by nebula shocks.

2.4. *Timing of Surface Density Constraints*

The power-law fit we have derived to the solar nebula surface density appears applicable across a large range of radii, from the 2–3 AU region where chondrules formed to about 30 AU, the distance out to which Neptune migrated. The surface density inferred from chondrule formation refers to the density of *gas* in the 2–3 AU region, at the time that the chondrules formed. For most chondrules this is inferred to have taken place approximately 1–3 Myr after the formation of calcium-rich, aluminum-rich inclusions (CAIs), which themselves probably formed within the first $\approx$1 Myr of the solar nebula (Wadhwa et al. 2007). The surface density we infer for the 2–3 AU region therefore only applies at a particular time, about 2 Myr (perhaps 1–3 Myr) into disk evolution.

The constraints arising from the augmented masses are different. By definition, these augmented masses refer to planetesimals, solids in the form of particles large enough to dynamically decouple from the gas (roughly tens of meters). As such, these augmented masses reflect the surface density of the solar nebula at a particular time, which is the time at which solids grew to planetesimal sizes. After dynamically decoupled planetesimals form, the gas can evolve, dissipate, even disappear, and it will not alter the distribution of planetesimals. In fact, this is exactly what is assumed to have happened with regard to the planetesimal disk, which must have been in place at the time of the 2:1 resonance crossing, far too late in disk evolution for gas to persist. The timing of the surface density constraints from the augmented masses can be considered a snapshot of the density of gas and solids, *at the time that the planetesimals formed*.

We regard the simulations of cometesimal growth by Weidenschilling (1997) to be particularly relevant to determining the timing of this snapshot of disk evolution. Weidenschilling (1997) examined coagulation of dust into larger bodies at 30 AU, using a density of solids $\rho_{\rm solids} = 4.2 \times 10^{-15}$ g cm^{-3}. Using our inferred density (eq. [5]), we estimate an initial dust density 6.5×10^{-15} g cm^{-3} at 30 AU, only slightly higher. Given the similar conditions, we expect the results to be applicable to the disk considered here. In those simulations, centimeter-sized particles grow by 0.06 Myr, and meter-sized bodies by 0.07 Myr. During this time interval, near collisional equilibrium is established, with erosion of meter-sized bodies replenishing dust as it coagulates into larger particles. Some fraction of the large bodies continue to grow, however. By 0.1 Myr, a considerable fraction of the mass is in bodies 10–100 m in size, and in bodies 100 m–1 km in size by 0.2 Myr. After 0.25 Myr, a large reservoir of bodies with diameters of about 100 m coexists with dust and large bodies >10 km in diameter. For the largest bodies only, gravitational focusing becomes important, and they undergo runaway growth. The order of events is not significantly different at other locations in the solar nebula but would proceed much more quickly. As reviewed in Weidenschilling (2000), the timescale for forming planetesimals at any location is about a few thousand times the local orbital period: 2000 yr at 1 AU, 3×10^5 yr at 30 AU. The surface densities in our model are higher than the densities considered by Weidenschilling (1997), by factors of a few, so one might expect particle growth to be even faster. We conclude that the surface density we have derived is a snapshot of the nebula at very early times, no later than about 0.3 Myr at 30 AU, and perhaps $\sim 10^4$–10^5 yr at 5 AU.

3. IMPLICATIONS FOR DISK EVOLUTION

In the previous section we used the augmented masses of the planets, along with other constraints to infer a surface density profile of the solar nebula. This surface density profile is well approximated by a power law with radius, $\Sigma(r) = \Sigma_0 (r/10\ {\rm AU})^{-p}$, with $p \approx 2.168$, and $\Sigma_0 = 343 (f_p/0.5)^{-1}$ g cm^{-2}. It is assumed in deriving this profile that the giant planets achieved their isolation masses. To test the validity of this assumption, it is necessary to construct models for the evolution of the protoplanetary disk and the growth of planets within it. In this section we construct evolutionary models of the solar nebula.

3.1. *Alpha Disks*

Constructing a model for the origin and evolution of our inferred surface density profile is a theoretical challenge. Most models predict $\Sigma(r) \propto r^{-1}$, not a profile as steep as the one we infer, $r^{-2.168}$. Unfortunately, the physical process by which mass and angular momentum are transported through protoplanetary disks, thereby allowing them to evolve, has never been identified positively. Among the promising mechanisms suggested by Stone et al. (2000) are gravitational instabilities and magnetohydrodynamic turbulence triggered by the magnetorotational instability. To date there are no simulations that can follow the evolution of a disk subject to any of these mechanisms for several Myr, and disk evolution models are necessarily phenomenological. It is standard to assume that the angular momentum transport is mediated by a local viscous shear, with effective viscosity ν. Under the α viscosity prescription, $\nu = \alpha c_s^2/\Omega$, where c_s is the local sound speed and Ω is the orbital frequency (Shakura & Sunyaev 1973). Assuming a single value of α throughout the disk is clearly an oversimplification of disk evolution but does allow long-term evolutionary models to be constructed. It does seem that the gross features of disk evolution via gravitational instability can be captured by models with $\alpha \sim 10^{-2}$ (Gammie 2001; Boley et al. 2007), and disk evolution by magnetorotational instability is also adequately described by α models (Stone et al. 2000). It is also possible to parameterize the viscosity using the β viscosity formalism in which $\nu = \beta r^2 \Omega$ (Dubrulle 1993). This formalism is based on the idea that viscous transport is mediated by turbulence generated by differential rotation and is formally independent of temperature, in contrast to the α disk model. However, in a Keplerian disk with $\Omega \propto r^{-3/2}$, the α formalism predicts $\nu \propto T(r) r^{3/2}$ while the β formalism predicts $\nu \propto r^{1/2}$, so the two approaches could be made exactly equivalent by assuming a temperature that varies as $T(r) \propto r^{-1}$. The α disk formalism has many drawbacks, yet it remains the most effective means of developing a simple model of disk evolution, glossing over the exact mechanisms that cause angular momentum to be transported. The two models we develop in this section are based on an α viscosity.

To develop such models, it is necessary to first constrain α and the temperature profile of the disk. In regions of the disk that are not actively accreting, the temperature will be set by the absorption of starlight and emission of radiation, and $T(r)$ is relatively insensitive to the dynamics and structure of the disk. Throughout this paper we adopt the temperature profile of Chiang & Goldreich (1997), $T(r) = 150 (r/1\ {\rm AU})^{-0.429}$ K. It is beyond the scope of this paper to attempt to construct self-consistent temperature profiles using our inferred surface density profiles, and this formula is expected to yield a reasonable approximation to the temperature in the disk. For example, observations of emission from protoplanetary disks support $T(r) \propto r^{-q}$ with $q \approx 0.5$ (Kenyon & Hartmann 1995). The value of α can be estimated in several ways. Observations of viscous disk spreading in protoplanetary disks in the Taurus molecular cloud suggest that $\alpha \sim 10^{-2}$ yields an appropriate magnitude of the viscous timescale in those disks (Hartmann et al. 1998). In their analysis of DM Tau and GM Aur, Hueso & Guillot (2005) similarly inferred α in the range 10^{-4} to 10^{-2}. A direct estimate of α in the solar system (at least in one time and place) comes from the size sorting of chondrules in chondrites by turbulence. The chondrules that are sorted have a product of ρ_c and radius a_c (i.e., aerodynamic stopping time) proportional to the level of turbulence. Working from Cuzzi et al. (2001), the appropriate value of α is

$$\alpha = \left(\frac{\rho_g}{\rho_c a_c} \right)^2 \frac{\nu_m}{\Omega}, \tag{6}$$

where ν_m is the molecular viscosity. The molecular viscosity of hydrogen gas is a measured quantity and can be estimated using

Sutherland's formula. We first calculate the viscosities η of H_2 and He gases:

$$\eta = \frac{\eta_0}{\rho_g}\left(\frac{T_0 + C}{T + C}\right)\left(\frac{T}{T_0}\right)^{3/2}, \quad (7)$$

where $\eta_0(T_0 + C)T_0^{-1.5} = 6.5 \times 10^{-7}$ (cgs units) and $C = 71$ K for H_2 gas, and where $\eta_0(T_0 + C)T_0^{-1.5} = 1.52 \times 10^{-7}$ (cgs units) and $C = 98$ K for He gas (Lide 1992). The viscosities then add reciprocally, weighted by the mole fraction of each gas:

$$\frac{1}{\eta} = \frac{X_{H_2}}{\eta_{H_2}} + \frac{1 - X_{H_2}}{\eta_{He}}, \quad (8)$$

where $X_{H_2} = 0.818$ for a solar composition gas. Finally, $\nu_m = \eta/\rho_g$. Assuming $\rho_g = 1.05 \times 10^{-9}$ g cm^{-3} and $T = 100$ K at 2.5 AU, we calculate $\eta = 42$ μP and $\nu_m = 4.0 \times 10^4$ cm^2 s^{-1}. The observed range of $\rho_c a_c$ for chondrules is 0.015–0.15 g cm^{-2} (Cuzzi et al. 2001), or 0.047 g cm^{-2} give or take a factor of 3. Combining these results, we infer a most likely value for $\alpha = 3.8 \times 10^{-4}$, with a possible range $\alpha \approx 4 \times 10^{-5}$ to 4×10^{-3}, in the chondrule-forming region. At least in the time and place of chondrule formation (i.e., 1–3 Myr into disk evolution, at the disk midplane about 2–3 AU from the Sun), $\alpha \approx 4 \times 10^{-4}$. Clearly a large range of α could be considered reasonable, with values in the range $10^{-4} < \alpha < 10^{-2}$ apparently most likely. Assuming α in this range, and using the temperature profile of Chiang & Goldreich (1997), we now construct disk evolution models.

3.2. *Viscously Spreading Disks*

The evolution of a viscously spreading disk has been considered by Lynden-Bell & Pringle (1974) and Pringle (1981) in the context of α viscosity, and more recently by Davis (2003, 2005) in the context of a β viscosity. In a viscously spreading disk, conservation of mass and angular momentum, together with the definition of a viscous torque, leads to the following solution for the time-dependent surface density profile:

$$\Sigma(r, t) = \text{const}\left(\frac{r}{r_0}\right)^{-(3/2-q)} T^{-(q+1)/(q+1/2)} \times \exp\left[-\frac{(r/r_0)^{(q+1/2)}}{T}\right], \quad (9)$$

where

$$T = 1 + 3\left(q + \frac{1}{2}\right)^2 \frac{\nu(r)t}{r^2}. \quad (10)$$

An α viscosity has been assumed here, with $T \propto r^{-q}$. A very similar formula was derived by Davis (2003) assuming a β viscosity and can be recovered here by setting $q = 1$ and adjusting constants appropriately. At late times ($T \gg 1$), $\Sigma(r, t)$ evolves to a profile like $r^{-(3/2-q)}$, which, if $q \approx \frac{1}{2}$, means that $\Sigma(r) \propto r^{-1}$. Because angular momentum is conserved within a viscously spreading disk, any mass that is accreted onto the star must give up its angular momentum to mass farther from the star; this mass then is forced to orbit at higher radii. In other words, while the inner parts of a viscously spreading disk may accrete inward, the outer parts of the disk must expand outward. The transition radius between inward and outward net mass flow is given by

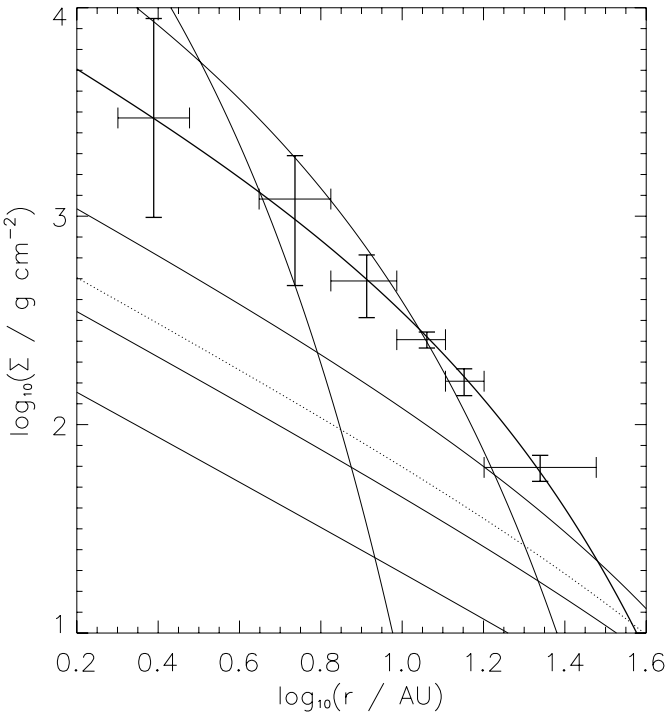

FIG. 2.—Surface density of gas in a viscously spreading disk. Crosses are as in Fig. 1. The lines represent the surface densities at various dimensionless times T, as in eq. (9). Assuming $\alpha = 3 \times 10^{-3}$, these correspond to physical times (*top to bottom*) 0, 0.1, 0.3 (*in bold*), 1, 2 (*dotted*), 3, and 10 Myr. While an instantaneous match to the surface density profile can be found, the gas density rapidly decreases afterward.

$$R_t(t) = r_0\left[\frac{T}{2(q + 1/2)}\right]^{1/(q+1/2)} \quad (11)$$

and moves outward over time.

The surface density profile of equation (9) provides an adequate match to our inferred surface density (eq. [4]) by a judicious choice of r_0 and T. Without delving into the details, these values are found by fitting the slope of our inferred profile at the location where Uranus formed. It is readily found that the optimal match is found at $T = 9.95$. This solution is displayed in Figure 2 for various values of T; the solution with the optimal value of $T = 9.95$ is displayed in bold.

The mass of this disk is $0.033(f_p/0.5)^{-1}$ $M_\odot$. At the time of this match, the transition radius is predicted to lie at about 6 AU.

Because of the self-similar nature of the solution of Lynden-Bell & Pringle (1974), the match corresponds only to a dimensionless time T; this can be converted to a physical time by the proper selection of α. Setting $T = 9.95$ and adopting $T(r) = 150(r/1\text{ AU})^{-0.429}$ K, we find that the physical time of optimal match is

$$t_{\text{match}} = 0.3\left(\frac{\alpha}{3 \times 10^{-3}}\right)^{-1} \text{ Myr}. \quad (12)$$

As discussed in § 2.4, our inferred surface density profile is measuring the spatial distribution of planetesimals at the time they dynamically decoupled from the gas. Since even at 30 AU planetesimals should have grown to the necessary size within 0.3 Myr, this implies that $\alpha \geq 3 \times 10^{-3}$. This value of α is within the acceptable range but implies a very rapid evolution of the disk.

It is an inescapable feature of viscously spreading disks that they evolve very rapidly, probably too rapidly to be consistent with the many constraints on disk evolution and planet formation. For one thing, it is unlikely that planetesimals formed and decoupled from the gas simultaneously at all the planets' locations; according to Weidenschilling (1997), planetesimals at 10 AU should have formed within 0.003 Myr, while those at 30 AU should have taken 0.3 Myr to form. But at 0.003 Myr, when planetesimals should have formed at 10 AU, the viscously spreading disk model predicts densities that are over an order of magnitude lower than the augmented mass of Saturn would imply. It is not at all clear that a viscously spreading disk model can match the surface density of equation (4) at early times at small r and at later times at large r.

Another problem with the viscously spreading disk model is that, following the formation of planetesimals in the region where gas giant planets formed, the gas is lost very rapidly. Specifically, in the Uranus-forming region at 14.2 AU, the gas density drops by a factor >10 after 10 Myr. As we discuss in the following section, gas damps the eccentricities of planetesimals, allowing them to accrete more rapidly, but if this gas is absent, then the formation of Uranus within the lifetime of the disk is frustrated. Finally, it is clear that in the time and place where chondrules formed (1–3 Myr after the formation of the solar system, at $r \approx$ 2–3 AU), a viscously spreading disk model predicts gas densities an order of magnitude too low to explain chondrule formation by nebular shocks (Fig. 2, *dotted line*).

The multiple constraints on the surface density of the solar nebula apply at various times in the disk's evolution: the constraints from planetesimals apply at various times, from $<10^4$ yr to perhaps 0.3 Myr, while the constraint from chondrule formation applies at 1–3 Myr. If a disk evolving by viscous torques is to satisfy all of these conditions, then it seems necessary for the disk to remain in a steady state configuration for several million years and not spread out viscously as in the model of Lynden-Bell & Pringle (1974).

3.3. *Steady State Disks*

At first glance, a steady state α disk with a surface density profile as steep as we infer [$\Sigma(r) \propto t^{-2.168}$] seems impossible. To see why, it is necessary to briefly review disk dynamics. A disk evolving by viscous torques must conform to two differential equations describing conservation of mass and angular momentum:

$$\frac{\partial \Sigma}{\partial t} = \frac{1}{2\pi r}\frac{\partial \dot{M}}{\partial r} \tag{13}$$

and

$$\frac{\partial}{\partial t}\left(\Sigma r^2 \nu\right) = \frac{1}{r}\frac{\partial}{\partial r}\left(\frac{\dot{M}}{2\pi} r^2 \Omega + r^3 \Sigma \nu \frac{\partial \Omega}{\partial r}\right) \tag{14}$$

(Lynden-Bell & Pringle 1974). Here $\dot{M}$ is the net flow of mass through any annulus, with $\dot{M} > 0$ describing inward accretion and $\dot{M} < 0$ describing outward flow. In a steady state disk the time derivatives in these equations vanish, which immediately yields the requirement that $\dot{M}$ be uniform in r (although it should be noted that the sign of $\dot{M}$ is unconstrained). Integration of equation (14) then yields

$$\frac{-\dot{M}}{2\pi} r^2 \Omega - r^3 \Sigma \nu \frac{\partial \Omega}{\partial r} = \text{const.} \tag{15}$$

The constant can be evaluated by application of an appropriate boundary condition. Typically it is assumed that mass flows toward the star, its orbital frequency increasing as $\Omega \approx (GM_\star/r^3)^{1/2}$ as it approaches the star. The gas is assumed to accrete onto the star in a thin boundary layer near the stellar surface, where its angular velocity is suddenly decreased from Keplerian rotation to stellar rotation rates, by additional, unspecified forces. In this scenario it is necessarily the case that $\partial\Omega/\partial r = 0$ at $r \approx R_\star$. At that location, const $= (-\dot{M}/2\pi)(GM_\star R_\star)^{1/2}$, yielding a solution for the surface density in a steady state Keplerian disk in which angular momentum is transported by viscous torques:

$$\Sigma(r) = \frac{\dot{M}}{3\pi\nu(r)}\left[1 - \left(\frac{R_\star}{r}\right)^{1/2}\right]. \tag{16}$$

Neglecting the term of order $(R_\star/r)^{1/2}$,

$$\Sigma(r) \approx \frac{\dot{M}}{3\pi\nu(r)}. \tag{17}$$

This is the structure of a large, steady state Keplerian disk that is often quoted (Lynden-Bell & Pringle 1974; Pringle 1981). In such a steady state disk, $\Sigma(r) \propto \nu^{-1}$, so assuming an α viscosity, $\Sigma(r) \propto r^{-(3/2-q)}$. Existing steady state α disk models would therefore predict $p = 3/2 - q \approx 1$ and would exclude $p = 2.168$.

We now report on a new solution for protoplanetary disk structure evolving by viscous torques. Specifically, we revisit the assumption that disks evolve because of an inner boundary condition. It was only because of the assumption of accretion onto the star via a boundary layer at this inner radius that the term like $r^{-1/2}$ was neglected. The application of an inner boundary is dubious because it assumes that accretion extends all the way to the star's corotation radius. If, for example, mass was drained from the disk by stellar magnetospheric accretion, at the corotation radius (Königl 1991), there would be no maximum in $\Omega(r)$, and the inner boundary condition would be severely modified. We now proceed to solve the steady state equations (13) and (14) without applying this inner boundary condition and ask what conditions are necessary to have a surface density profile $\Sigma(r) \propto r^{-p}$ with $p \approx 2.168$.

Solving equations (13) and (14) assuming an α viscosity $\nu = \alpha c_s^2/\Omega$ with $T(r) \propto r^{-q}$ yields

$$\Sigma(r) = \frac{\dot{M}}{3\pi\nu(r_0)}\left(\frac{r}{r_0}\right)^{-(3/2-q)} + \frac{\dot{m}}{3\pi\nu(r_0)}\left(\frac{r}{r_0}\right)^{-(2-q)}, \tag{18}$$

where $\dot{M}$ measures the mass flux as before and $\dot{m}$ and r_0 are convenient constants. In this *more general* solution to the disk evolution equations, the signs of neither $\dot{M}$ nor the constant of integration $\dot{m}$ are constrained. Note, however, that they cannot both be negative (because then $\Sigma < 0$). The steepness of this density profile is readily found by evaluating

$$p = -\frac{\partial \ln \Sigma}{\partial \ln r} = \frac{2 - q + x(3/2 - q)}{1 + x} = \frac{3}{2} - q + \frac{1/2}{1 + x}, \tag{19}$$

where $x \equiv (\dot{M}/\dot{m})(r/r_0)^{1/2}$. The standard inner boundary condition assumption amounts to neglecting $\dot{m}$ in favor of $\dot{M}$, or equivalently $|x| \gg 1$, so that $\dot{M} = 3\pi\Sigma\nu$ and $p \rightarrow 3/2 - q$ as before. If $\dot{M}$ and $\dot{m}$ have the same sign, then $x > 0$ and $p \leq 2 - q$, which is still incompatible with our inferred surface density with slope

$p = 2.168$. But if $\dot{M}$ and $\dot{m}$ have opposite signs, so that $x < 0$, it is possible to have $\Sigma > 0$ and $p > 2$. By solving for $\dot{m}$, we find

$$\dot{m} = \frac{p + q - 3/2}{2 - p - q} \left(\frac{r}{r_0}\right)^{1/2} \dot{M}. \quad (20)$$

On substitution of $\dot{m}$ into equation (18), this yields

$$\dot{M} = -2[p(r) + q - 2]3\pi\nu(r)\Sigma(r). \quad (21)$$

Of course, the forms of $p(r)$ and $\Sigma(r)\nu(r)$ combine so that $\dot{M}$ is uniform throughout the relevant regions of the disk, as required for a steady state disk. Now it is readily seen that in regions of the disk where $p(r) + q > 2$, $\dot{M} < 0$ and the flow is outward, a condition previously derived by Takeuchi & Lin (2002). For the slope $p = 2.168$ we derive in our fit, it *must* be the case, at least in a steady state α disk, that $\dot{M} < 0$ and mass accretion is outward.

By assuming $\dot{M} < 0$ and retaining both terms in the steady state surface density profile, an extremely good match to our inferred surface density profile can be found. If we force the general solution to equation (18) to have slope p at a location r_U, it must assume the form

$$\Sigma(r) = \frac{\Sigma_U}{1 + x_U} \left(\frac{r}{r_U}\right)^{-(2-q)} \left[1 + x_U \left(\frac{r}{r_U}\right)^{1/2}\right], \quad (22)$$

where $x_U = -(p + q - 2)/(p + q - 3/2)$. We fix $p = 2.168$ and $q = 0.429$, yielding $x_U = -0.544$. We then optimize the two remaining parameters and find $r_U = 18.0$ AU and $\Sigma_U = 95.94 \times (f_p/0.5)^{-1}$ g cm^{-2}. This solution is displayed in Figure 1 as the thick solid line. This profile fits the surface density constraints very well; again treating the uncertainties as standard deviations, we derive $\chi^2_\nu = 0.08$.

An interesting and inevitable feature of our steady state disk model is that the surface density must vanish at an outer edge, $r_d = r_U x_U^2$. By matching the double power-law profile to equation (4) at $r_U = 18$ AU, this edge is found to lie at 61 AU. Because the location of the edge is proportional to r_U, we do not consider our model able to predict where the edge of the disk should lie exactly within a broad range from about $x_U^{-2}(10\text{–}30\ \text{AU}) \approx 30\text{–}100$ AU. On the other hand, our inferred distribution of mass is wholly consistent with the Kuiper Belt having an edge at 45–50 AU and provides insight into why.

We now return to the physical context for our steady state solution. It is characterized by an outward mass flux, with the surface density vanishing at an outer boundary. Some mechanism must deplete the disk of mass, at a rate $\dot{M}$. The obvious candidate for this mechanism is photoevaporation by an external massive star (Hollenbach et al. 2000; Hollenbach & Adams 2004; Adams et al. 2004). The physics of external photoevaporation of protoplanetary disks has been studied by Adams et al. (2004). Essentially, far-ultraviolet (FUV) radiation from nearby massive stars heats gas at the disk periphery and increases its sound speed. Beyond a radius $r_g \sim 100$ AU, the sound speed exceeds the escape velocity directly and the gas is rapidly depleted. As the disk shrinks to sizes $r_d \ll r_g$, further photoevaporation at a reduced rate is still possible. Most of the gas is depleted from the outer edge of the truncated disk, at r_d. The evaporative mass-loss rate has been tabulated by Adams et al. (2004) as a function of the FUV flux (parameterized by G_0) and disk radius r_d.

It is the nature of photoevaporation to create a high-temperature, high-pressure ring of gas at r_d, at the outer edge of the disk. The radial extent of this heated region is Δr, where $\Delta r \ll r$ owing to the high optical depths to FUV radiation in the disk. Gas orbiting at $r < r_d - \Delta r$ is in Keplerian rotation, with $\Omega_K = (GM_\star/r^3)^{1/2}$, decreasing with increasing radius. Gas orbiting at $r_d - \Delta r < r < r_d$, on the other hand, experiences an additional inward force due to the steep pressure gradient within the heated zone. Balancing the forces on the gas, one finds

$$\Omega^2 r = \Omega_K^2 r + \frac{1}{\rho}\frac{\partial P}{\partial r}, \quad (23)$$

where P is the pressure. Throughout much of the Keplerian disk, pressure decreases with increasing radius, causing gas to orbit at a rate $\Omega < \Omega_K$ slower than Keplerian rotation, as is well known (Weidenschilling 1977b). Within the photoevaporating annulus, however, P increases with radius, causing the gas to rotate faster than Keplerian.

The effect of the pressure gradient is significant because its magnitude is $\partial P/\partial r \sim \rho C_{\rm evap}^2/\Delta r$, where $C_{\rm evap}$ ($\sim$few kilometers per second) is the sound speed of the photoevaporating gas. Within the photoevaporating annulus, the magnitude of Ω is

$$\Omega^2 \sim \Omega_K^2 \left(1 + \frac{r}{\Delta r}\frac{C_{\rm evap}^2}{r^2\Omega_K^2}\right). \quad (24)$$

While $C_{\rm evap} \sim r\Omega_K$, $r \gg \Delta r$, so the orbital frequency of the gas must *increase*, significantly, in the photoevaporating region at the disk boundary, r_d. This has two important consequences for disk evolution. First, gas must gain substantially more angular momentum to cross r_d into the photoevaporating region than it would if it were in an isolated, viscously spreading disk. This substantially reduces the ability of gas to flow past r_d, essentially limiting the mass flux to that which can be carried by photoevaporation. Second, a minimum in Ω^2 must exist just inside the disk radius. We use the fact that $\partial\Omega/\partial r = 0$ at the outer boundary r_d to reevaluate the constant in equation (15). The result is

$$\Sigma(r) = \frac{(-\dot{M})}{3\pi\nu(r)} \left[\left(\frac{r_d}{r}\right)^{1/2} - 1\right]. \quad (25)$$

This is exactly analogous to the circumstellar decretion disk solution discussed by Lee et al. (1991). Obviously steady state physical solutions exist for $r < r_d$ only if $\dot{M} < 0$ and mass is moving outward to replenish the mass lost due to photoevaporation. This solution is exactly equivalent to the solution presented in equation (22), provided that $x_U = -(r_U/r_d)^{1/2}$. Given the value of q and the slope p at $r_U = 18$ AU, the value of x_U is fixed at -0.544, leading to $r_d = 61$ AU. As already discussed, we do not consider r_d to be constrained except to a broad range $\approx$30–100 AU. It is nevertheless notable that the observed edge of the Kuiper Belt at 47 AU (Trujillo & Brown 2001) is within this range and close to our estimate of 61 AU. Photoevaporation has been invoked before as the cause of the Kuiper Belt edge (Hollenbach & Adams 2004), and our analysis here suggests that photoevaporation was also responsible for shaping the distribution of mass in the outer solar system. Photoevaporation both limits the viscous spreading of the disk and imposes an outer boundary to the disk that completely changes the density profile.

3.4. *A Scenario for Disk Evolution*

With the simple assumption that the solar nebula experienced photoevaporation, it is natural to recover the ''double power solution'' of equation (25). With the appropriate choice of two parameters, a surface density profile $\Sigma(r)$ is obtained that almost exactly matches the surface density we infer for the solar nebula. It is also significant that our solution is a steady state solution. As long as it is established by the time the first planetesimals form, within $\sim 10^4$–10^5 yr, and is maintained thereafter, then it can satisfy the *timing* of all of the surface density constraints as well. We therefore favor the photoevaporated disk solution over the viscously spreading disk model. We now outline a comprehensive scenario for disk evolution, designed to test the validity of the assumption that the giant planets grew rapidly enough to achieve their isolation masses, and to determine whether Neptune and Uranus could have formed within the lifetime of the disk and accreted H and He gas.

We hypothesize that the solar nebula disk formed and began viscously evolving, but soon thereafter, within about 10^4–10^5 yr, the disk was exposed to intense FUV radiation from nearby OB stars and began photoevaporating at its outer edge. Mass flowed outward through the outer disk to replenish the mass lost to photoevaporation, and our steady state disk profile (eqs. [22] and [25]) was established. Wherever planetesimals had formed by this time, they were dynamically decoupled from the gas, and their spatial distribution, $r^{-2.168}$ (eq. [4]), remained frozen from that point on. Meanwhile, photoevaporation continued to erode the outer edge of the disk, to radii inside 60 AU, while planetesimals continued to form at increasing radii beyond 30 AU. Beyond some radius between 30 and 60 AU planetesimal formation was inhibited completely by loss of disk material by photoevaporation; presumably this radius is marked today by the edge of the Kuiper Belt at 47 AU. Throughout the outer solar nebula where the giant planets formed, the disk was characterized by an outward flow of mass in which the gas densities were maintained in steady state.

In § 4 we show that the cores of Jupiter and Saturn can grow in less than 2 Myr, but Neptune's takes 6 Myr and Uranus's about 10 Myr, presuming that the high densities inferred from our surface density profile can be maintained that long. There are three constraints that must be satisfied for this to occur. First, the reservoir of mass in the inner solar nebula must be large enough to supply the outer solar nebula and the photoevaporation front for 10 Myr. Second, the outward mass flux must not be so large that it drains this reservoir too quickly. Third, the photoevaporation front must not encroach too closely on the 10–15 AU region where Uranus and Neptune form. We now quantify these constraints.

We estimate the mass that can flow from inside 10 AU, through the 10–15 AU region, to the photoevaporation front, by assuming that the profile of equation (4), with $f_p = 0.5$, applies for radii $r \geq R_{\rm join}$, and that this profile smoothly joins a profile varying as r^{-1} for $r < R_{\rm join}$. At the time that planetesimals formed, $R_{\rm join} < 2$ AU by assumption. Taking $R_{\rm join} = 1$ AU yields a total mass between 0.1 and 10 AU of $0.101\ M_\odot$. Despite this high mass, this disk is not obviously gravitationally unstable: assuming $T(r) = 150(r/1\ {\rm AU})^{-0.429}$ K, the minimum value of the Toomre Q parameter in the disk at this time is $Q = C\Omega/\pi G\Sigma \approx 1.4$ at 1 AU. As the solar nebula evolves and mass is drained from the inner solar nebula, the total disk mass decreases and $R_{\rm join}$ increases. By the time $R_{\rm join}$ grows to 10 AU, the disk mass is found to decrease to $0.024\ M_\odot$. Because $R_{\rm join} < 10$ AU still, the surface density in the 10–15 AU region would not change as $R_{\rm join}$ increases from 1 to 10 AU, even as the region from 0.1 to 10 AU loses $0.077\ M_\odot$. Some of this mass must flow onto the central star, but a sizeable fraction of this lost mass also must flow outward. We estimate

$$M_{\rm rsrvr} \approx 0.05\left(\frac{f_p}{0.5}\right)^{-1} M_\odot \tag{26}$$

as the mass of the reservoir of gas available to move outward through the 10–15 AU region.

The uniform and constant mass flux through the outer solar nebula can be found using equation (21), evaluated at the location of Uranus:

$$\dot{M} = -1.3\times 10^{-9}\left(\frac{f_p}{0.5}\right)^{-1}\left(\frac{\alpha}{10^{-4}}\right) M_\odot\ {\rm yr}^{-1}. \tag{27}$$

The timescale for which mass flow can be maintained is therefore

$$t_{\rm flow} = \frac{M_{\rm rsrvr}}{-\dot{M}} \approx 40\left(\frac{\alpha}{10^{-4}}\right)^{-1}\ {\rm Myr}. \tag{28}$$

If the flow must be maintained for 10 Myr, an upper limit to α is 4×10^{-4}, corresponding to $\dot{M} = -5\times 10^{-9}\ M_\odot\ {\rm yr}^{-1}$.

This maximum allowed outward mass flux is surprisingly high and is comparable to the mass accretion rate onto T Tauri stars, but it does not violate constraints on the conservation of mass or energy. The typical mass accretion rates onto T Tauri stars follow a time variation

$$\dot{M}(t) \approx 1\times 10^{-8}\left(\frac{t}{1\ {\rm Myr}}\right)^{-1.40} M_\odot\ {\rm yr}^{-1} \tag{29}$$

(Hartmann et al. 1998). Integrating from 0.3 to 10 Myr yields a total mass of $0.031\ M_\odot$ that must accrete onto the central star. This is almost identical to the mass we have assumed accreted onto the Sun in our scenario outlined above ($0.027\ M_\odot$), so the expected mass in the inner solar nebula is sufficient to drive the outward mass flux. Using the starting profile outlined above, this $0.03\ M_\odot$ would extend from the disk inner edge to 1.0 AU. The $0.05\ M_\odot$ of gas flowing outward would originate from 1 AU and beyond. The gravitational binding energy and angular momentum released by the accretion of the gas inside 1 AU are more than sufficient to power the outflow of the gas beyond 1 AU.

Finally, we consider the constraints on the photoevaporation rate. Because the surface density profile reflects the presence of an outer boundary at the time planetesimals formed, the photoevaporation rate must have been sufficient to erode the disk down to 50 AU (the edge of the Kuiper Belt) on timescales $\sim$1 Myr. If the surface density of the outer nebula beyond 50 AU were known, it would be possible to constrain the strength of the photoevaporating radiation exactly. A minimum value can be determined by noting that to reach 50 AU photoevaporation must be capable of removing gas there at a rate of at least $-\dot{M}$. Figure 4 of Adams et al. (2004) reveals that if $\dot{M} = -5\times 10^{-9}\ M_\odot\ {\rm yr}^{-1}$, G_0 must exceed about 1000, which would place the Sun in a cluster of at least a few hundred stars (Adams et al. 2004). Higher values of G_0 are also allowed but could potentially erode the disk too close to the 10–15 AU region, thereby reducing the surface density of gas there. A reduction in r_d (in eq. [25]) from 60 to 30 AU would decrease Σ at 14.2 AU by a factor of 0.43; a reduction from 60 to 20 AU would decrease it by a factor of 0.18.

If the photoevaporation front is not to erode the disk inside of about 30 AU, G_0 must not exceed about 3000, at least during these later stages ($\approx$5–10 Myr) of disk evolution. Of course, higher values of G_0 are probably associated with very massive, nearby stars, which would go supernova within 4 Myr, before photoevaporation would approach 30 AU. Overall, it is difficult to place an upper limit on G_0 during the first few million years of disk evolution, but modest amounts of photoevaporation ($G_0 > 1000$) are demanded to understand the surface density of the solar nebula.

To summarize, very reasonable assumptions about disk properties lead to a model in which high densities of gas can be maintained in the region where giant planets formed, for up to 10 Myr. These assumptions include a moderately high disk mass $\sim$0.10 $M_\odot$ inside 10 AU, which is within the range of masses observed for protoplanetary disks (Eisner & Carpenter 2006), and which is not apparently gravitationally unstable. The disk is assumed to transport angular momentum by viscous torques with an effective $\alpha \approx 4 \times 10^{-4}$, which is also within the range of reasonable α. Most importantly, moderate amounts of photoevaporation are demanded, $G_0 \approx 3000$. This removes mass from the outer edge of the disk at a fixed rate and imposes our steady state solution on the disk surface density. This amount of photoevaporation is reasonable if the Sun was formed in a cluster (Adams et al. 2004).

4. IMPLICATIONS FOR TIMESCALES OF PLANET FORMATION

In the previous section we attempted to construct evolutionary models for the protoplanetary disk. Out of necessity, we modeled the disk as evolving due to viscous torques described using an α viscosity. Within the context of these disk models, we now model the growth of the giant planets. One of our goals is to ascertain whether all four giant planets can grow to their observed masses within the lifetime of the disk, especially so that Uranus can accrete H and He before the disk dissipates. A second goal is to test the fundamental assumption of MMSN models and our inferred surface density profile, that the giant planets achieved their isolation masses and accreted all of the planetesimals in their feeding zones.

In the standard MMSN, formation of even Jupiter, at 5 AU, is problematic. Models of its growth typically invoke enhanced surface densities of solids to form it within a few million years (e.g., Pollack et al. 1996; Chambers 2006). Growth of the cores of Uranus and Neptune is much slower at the locations where these planets formed, as the orbital frequencies and surface densities there are orders of magnitude smaller. In the context of the standard MMSN, formation of Uranus and Neptune within the lifetime of the disk is unexplained. However, the surface density we infer for the solar nebula is much higher than the traditional MMSN and much more conducive to planet formation. Integrating equation (4) over radius, we conclude that just between 2 and 30 AU the solar nebula must have contained $0.060(f_p/0.5)^{-1}$ $M_\odot$ of material, about 6 times the amount of mass between 2 and 30 AU in the standard MMSN (0.010 $M_\odot$). The surface density of large solids (planetesimals) that we infer in the region where Jupiter formed is roughly 9.6 g cm^{-2} (independent of f_p), also a factor of about 5 over the surface density of solids there in the standard MMSN. In this section we demonstrate that owing to the Nice model's more compact planetary configuration, and also because of the higher surface densities in the solar nebula this configuration implies, formation of *all* the giant planets is possible within the lifetime of the disk.

The growth rate of a core can be found assuming that it accretes planetesimals of mass m_p, each with a randomly oriented (in three dimensions) velocity of magnitude v with respect to the core. In that case

$$\frac{dM_c}{dt} = n_p m_p v_p \pi R_{\rm capt}^2 \left(1 + \frac{2GM_c}{R_{\rm capt} v_p^2}\right), \tag{30}$$

where the second term in parentheses accounts for gravitational focusing, and planetesimals are considered captured if they approach the core to within a distance $R_{\rm capt}$ from its center (e.g., Ida & Makino 1993). To evaluate this growth rate, the number density n_p and velocity v_p of planetesimals must be evaluated in terms of other quantities.

The velocities of planetesimals do not take on a single value but rather are distributed over a range, with a typical value being $v_p \sim \langle e^2 \rangle^{1/2} r\Omega$. It is also assumed that planetesimals are vertically distributed with scale height $\sim v_p/\Omega$, so that $n_p \approx \Sigma_p \Omega / v_p$, Σ_p being the surface density of planetesimals in the disk. [Note that $\Sigma_p = 2.56\ (r/10\ {\rm AU})^{-2.168}$ g cm^{-2} is independent of f_p.] Gravitational focusing usually enhances the collisional cross sections by factors $\gg 1$. Taking all of these approximations, the growth rate becomes

$$\frac{dM_c}{dt} \approx C\pi\Sigma_p \frac{2GM_c R_{\rm capt}}{\langle e^2 \rangle^{1/2} r^2 \Omega} \tag{31}$$

(Ida & Makino 1993; Kokubo & Ida 2002), where $C \approx 2$ (Ida & Nakazawa 1989) is a numerically determined factor that accounts for the increased probability of collision as planetesimals execute complicated orbits inside the core's Hill sphere. This is the growth rate we utilize here, to determine whether cores can grow within about 10 Myr.

A needed input to this formula is the rms eccentricity of the planetesimals, $\langle e^2 \rangle^{1/2}$, which is determined by a balance between gravitational stirring by the planetary core (which increases $\langle e^2 \rangle^{1/2}$) and drag forces by the gas in the solar nebula (which reduce $\langle e^2 \rangle^{1/2}$). This equilibrium value has been determined by Kokubo & Ida (2002), who find $\langle e^2 \rangle^{1/2} = (M_c/3\ M_\odot)^{1/3} \langle \tilde{e}^2 \rangle_{\rm eq}^{1/2}$, where

$$\langle \tilde{e}^2 \rangle_{\rm eq}^{1/2} = 5.6 \left(\frac{m_p}{10^{23}\ {\rm g}}\right)^{1/15} \left(\frac{\rho_p}{2\ {\rm g\ cm^{-3}}}\right)^{2/15} \left(\frac{\tilde{b}}{10}\right)^{-1/5} \times \left(\frac{C_D}{1}\right)^{-1/5} \left(\frac{\rho_{\rm gas}}{2 \times 10^{-9}\ {\rm g\ cm^{-3}}}\right)^{-1/5} \left(\frac{r}{1\ {\rm AU}}\right)^{-1/5}. \tag{32}$$

Here ρ_p is the planetesimals' internal density, $\tilde{b}$ is the mean separation of protoplanets in units of their mutual Hill radii, C_D is the drag coefficient relevant to the planetesimals, $\rho_{\rm gas}$ is the gas density, and r is the heliocentric distance. Because we are most interested in understanding the formation of Uranus and Neptune, we adopt $\tilde{b} = 7.0$ in what follows (the starting separation of Uranus and Neptune in units of their mutual Hill radius). The drag coefficient can be estimated by first finding the particle Reynolds number ${\rm Re}_p = 2v_{\rm rel}R_p/\nu_m$, where $v_{\rm rel} \sim \langle e^2 \rangle^{1/2} r\Omega$ is the relative velocity between the planetesimal and the gas, R_p is the planetesimal's radius, and ν_m is the molecular viscosity of the gas (eq. [7]). In terms of ${\rm Re}_p$, we follow Weidenschilling (1977b) and set $C_D = 24{\rm Re}_p^{-1}$ for ${\rm Re}_p < 1$, $C_D = 24{\rm Re}_p^{-0.6}$ for $1 < {\rm Re}_p < 785$, and $C_D = 0.44$ for ${\rm Re}_p > 785$. Even for the smallest planetesimals we consider here (100 m radius), the densities are high enough that $C_D = 0.44$ almost always.

Before using this formula, it is important to appreciate its limitations. Kokubo & Ida (2002) used this formula to estimate a timescale to grow to core mass M_c as $t_{\rm grow} \sim M_c/(dM_c/dt)$. This underestimates the actual growth timescale by a factor of 3 because $dM_c/dt \propto M_c^{2/3}$. We do not use this simplification; when we refer to growth timescales, they are the actual times at which the cores have accreted a total mass M_c. Even so, our calculations are uncertain to within factors of order unity because the growth rate formula contains uncertain factors of order unity, in the enhanced probability C, in the vertical distribution of planetesimals, and in the velocity dispersion of planetesimals. It is easy to imagine the growth timescales being a factor of 2 larger or smaller, and it is somewhat pointless to try to correct for these factors of order unity unless all such factors are corrected simultaneously. In addition, there are other physical effects not even accounted for in this formula that could change growth rates, such as the existence of a planetary atmosphere, which can enhance accretion rates (Inaba & Ikoma 2003). The tidal disruption of planetesimals near the core can also enhance the accretion rates. We are unaware of any attempts to quantify this effect, but we can estimate its importance here. The planetesimals being accreted by the planetary cores, if they are not identically comets, are at least likely to be comet-like. We assume that they are small (<1 km) and porous, with mean densities ≈ 0.5–1 g cm^{-3} and negligible internal strength, very similar in properties to comet Shoemaker-Levy 9 (Asphaug & Benz 1994). Like Shoemaker-Levy 9, these planetesimals will be tidally disrupted as they enter the tidal radius of the growing planetary core,

$$R_{\rm tidal} = R_c \left(\frac{2\rho_c}{\rho_p}\right)^{1/3} \approx 1.73 \left(\frac{\rho_c}{1.3\ {\rm g\ cm^{-3}}}\right)^{1/3} \left(\frac{\rho_p}{0.5\ {\rm g\ cm^{-3}}}\right)^{-1/3} R_c. \quad (33)$$

We assume, for the sake of simplicity, that 100% of planetesimals that approach to within a minimum distance r of the planetary core are accreted if $r \leq R_c$, and 50% of their mass is accreted if $R_c < r < R_{\rm tidal}$. The effective capture radius is then

$$R_{\rm capt} = R_c \left[1 + 0.5\left(\frac{R_{\rm tidal}^2}{R_c^2} - 1\right)\right]^{1/2}, \quad (34)$$

or about $1.41R_c$ for our assumed densities. Tidal disruption of bodies enhances the growth rate and reduces the growth timescales by about 40%. We do include the effects of tidal disruption, but undoubtedly there are other equally important factors we are not considering, and we cannot constrain the growth timescales to within factors of perhaps 2.

We have solved for $M_c(t)$ at different locations in the nebula, using our assumed surface density of planetesimals, $\Sigma_p = 2.56(r/10\ {\rm AU})^{-2.168}$ g cm^{-2}, and a surface density of gas $343(f_p/0.5)^{-1}(r/10\ {\rm AU})^{-2.168}$ g cm^{-2}, with $f_p = 0.5$. In these calculations, we have related the core radius to its mass assuming a density $\rho_c = 1.3$ g cm^{-3}. The planetesimals have assumed density $\rho_p = 0.5$ g cm^{-3}. In this calculation they also have a common radius of 100 m. The results are shown in Figure 3, which also delineates the range of core masses inferred for each planet (§ 2.3) and therefore the time taken for these cores to form.

Using these parameters, we calculate growth times of about 0.5 Myr for Jupiter, 1.5–2.0 Myr for Saturn, 5.5–6.0 Myr for Neptune, and 9.5–10.5 Myr for Uranus. These results are not to be considered final, given the uncertainties in the input parameters, not to mention the factors of order unity in the formula (eq. [31]). One of the largest uncertainties, and one to which the calculation is sensitive, is the size of the accreting planetesimals. The value of $R_p = 100$ m was chosen to represent the size of planetesimals—essentially comets—in the 10–15 AU region, but clearly $R_p \sim 1$ km could be considered equally reasonable. Had we chosen a planetesimal radius of 1 km, Saturn's core would take 4 Myr to form, that of Neptune about 15 Myr, and Uranus's much longer than that. The timescales are also sensitive to $\tilde{b}$ and to the assumed densities. Our purpose here is *not* to conduct a parameter study and outline all possible outcomes. Rather, we intend only to show that for a combination of reasonable parameters, using existing theory, growth of *all* the giant planets is possible within 10 Myr.

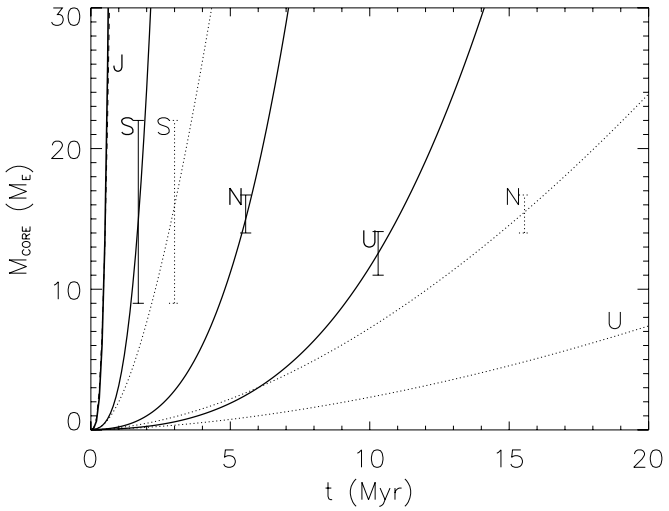

FIG. 3.—Core masses as a function of time. The masses of four planetary cores, at 5.45, 8.18, 11.5, and 14.2 AU (*left to right*), are shown, representing the cores of the planets Jupiter, Saturn, Neptune, and Uranus, respectively. Vertical bars represent the estimated core masses of Saturn, Neptune, and Uranus; their placements at various times are only to guide the eye. The masses of the cores of Jupiter, Saturn, Neptune, and Uranus reach their present-day values within 0.6, 2, 6, and 10 Myr, respectively, assuming that the surface densities in each location are maintained for as long as they take to form (*solid lines*). If the nebula is allowed to viscously spread, formation times are greatly prolonged as the lower gas densities fail to damp the eccentricities of planetesimals (*dotted lines*).

Using these same parameters, we can estimate the final masses of solids, M_Z, that each planet will attain, assuming that the surface densities of gas and solids are maintained. Figure 4 shows that after 10 Myr, cores can readily grow to $\sim 10\ M_\oplus$ inside of about 15 AU.

Inside about 15 AU, growth is so rapid, in fact, that cores exhaust all of the planetesimals in their feeding zones. Figure 4 plots (as the line labeled "$M_{\rm iso}$") the total mass of planetesimals in each planet's feeding zone, using the starting locations of the planets from the Nice model and our inferred surface density (eq. [4]). The inferred range of M_Z for each planet (§ 2.3) is also displayed. In each case, the mass M_Z is comparable to, but does not exceed, the mass of planetesimals in each planet's feeding zone. This implies that the giant planets grew quickly and consumed nearly all the planetesimals in their feeding zones.

The formation of all of the giant planets within 10 Myr is made possible only because of the high gas densities that are maintained in the 10–15 AU region, as a result of the steady state disk profile we have derived. Had we assumed that our inferred surface density profile were not due to this steady state profile driven by photoevaporation, but was instead a snapshot in time

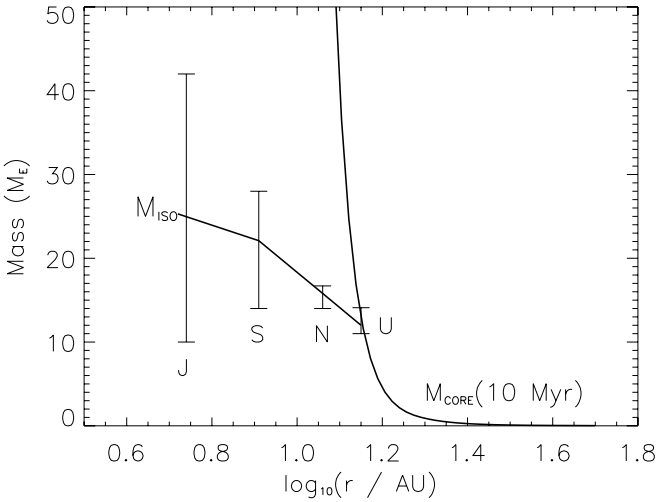

FIG. 4.—Final masses of solids in each planet. Assuming that the surface densities of gas and solids remain constant at our inferred values for 10 Myr, growth of a 10 $M_\oplus$ core within that time is predicted in each planet's feeding zone. The line shows the mass of core achieved after 10 Myr. Inside 15 AU, planetary growth is limited not by time constraints but by the availability of mass. The effective isolation mass, M_{iso}, is plotted for each planet's feeding zone. The vertical bars represent the total amount of solids (M_Z) inferred for each planet (including both cores and envelopes). The value of M_Z for each planet is consistent with the hypothesis that each planet exhausted the solids in its feeding zone during growth, justifying the assumption underlying the MMSN model.

of a viscously spreading disk, the formation of Uranus would take significantly longer than 10 Myr. Using the time-varying surface density profile of equation (9), assuming $\alpha = 3.0 \times 10^{-3}$ so that it matches the solar nebula at 0.3 Myr, we calculate that Neptune's core would take 3 times longer to form, about 15 Myr, and the core of Uranus would take about 30 Myr. These timescales are clearly incompatible with observations of disks, which show little gas present at these times (Haisch et al. 2001).

We do not address here the complicated question of accretion of gas onto the planetary cores. The critical mass onto which an atmosphere will start to accrete is usually taken to be $\sim 10\ M_\oplus$ (e.g., Pollack et al. 1996). Uranus reaches this mass at about 9 Myr, enjoys another 1 Myr of accretion of solids and gas, concurrently (e.g., Pollack et al. 1996) in the presence of the same initial high densities, and then experiences several million years of decreasing gas densities as the nebula finally dissipates. Future calculations would need to verify that retention of a few Earth masses of H-He gas can be accomplished during these few million years, but this seems like a very reasonable outcome. Retention of gas atmospheres would presumably be easier for the other planets.

To summarize, the starting locations of the planets from the Nice model, as well as the consequent surface density of gas and solids these new locations imply, paint the picture of a solar nebula disk far more conducive to planet formation than the standard MMSN disk. Disk models (§ 2) imply that this surface density could be consistent with either a viscously spreading disk with $\alpha \approx 3 \times 10^{-3}$ or a steady state photoevaporating disk with $\alpha \approx 4 \times 10^{-4}$. In either of these disks planet formation is much more rapid than previously calculated, but only in the photoevaporating disk is formation of Uranus possible within 10 Myr. A steady state, photoevaporating disk naturally yields a "double power-law" profile that very exactly conforms to the inferred surface density of the solar nebula. If it does indeed describe the structure of the solar nebula, then it is possible and in fact likely that the giant planets each achieved their isolation masses, validating this key assumption of the MMSN model.

5. DISCUSSION

The Nice model of solar system evolution (Tsiganis et al. 2005; Gomes et al. 2005; Morbidelli et al. 2005) explains many attributes of solar system architecture by positing that the giant planets formed in a much more compact configuration, from 5 to 15 AU, rather than where they are found today. Also central to the Nice model is the existence of a planetesimal disk of about 35 $M_\oplus$ extending from 16 to 30 AU. In this paper we have recalculated the distribution of mass in the solar nebula using these starting locations of the planets, from Gomes et al. (2005): Jupiter, 5.45 AU; Saturn, 8.18 AU; Neptune, 11.5 AU; and Uranus, 14.2 AU. From this we infer a near–power-law distribution of mass in the outer nebula, $\Sigma(r) = 343(f_p/0.5)^{-1} \times (r/10\ \mathrm{AU})^{-2.168}$ g cm^{-2}, where f_p is the fraction of the mass of solids that ended up in planetesimals decoupled from the gas.

5.1. *Conformance to a Single Trend*

We find that the distribution of mass conforms remarkably well to a single trend. This trend can be well approximated by a power law, $\Sigma(r) \propto r^{-2.168}$. Previous attempts to fit the giant planets did not reveal such good conformance to a power law, typically finding that the surface densities in the Uranus and Neptune regions were too low compared to the fit through the Jupiter and Saturn regions (W77). In contrast, our surface density derived from the augmented masses of all four giant planets conforms to a power law to within about 10%. A slightly better match is made assuming the double power-law steady state photoevaporating disk solution we have derived, which also fits to within 10%. Notably, the surface densities in the Uranus and Neptune regions *only* fit the overall trend if these two planets did indeed switch places when Jupiter and Saturn crossed their 2:1 MMR (a possibility to which Tsiganis et al. [2005] assign a 50% probability). This is very strong circumstantial evidence that for the first 15% of the solar system's history, Neptune was closer to the Sun than Uranus. Remarkably, three independent attributes of the planetesimal disk, derived from indirect dynamical constraints, also conform to the exact same trend. These are the average surface density from 16 to 30 AU, derived from the total mass of planetesimals that must be scattered in the context of the Nice model (Tsiganis et al. 2005); the surface density at the inner edge, which (once the outer radius of Uranus's feeding zone is established) is constrained by the timing of the LHB (Gomes et al. 2005); and the surface density at 30 AU, which is constrained by the fact that Neptune's migration halted there. The trend also predicts a surface density in the chondrule-forming region at 2–3 AU that is consistent with chondrule formation in nebula shocks.

It is also interesting to note that attempts to derive surface density profiles in extrasolar planetary systems also suggest profiles varying as $\Sigma \propto r^{-2}$ (Kuchner 2004), very similar to our inferred slope of -2.168. Likewise, the surface density of the sub-Jovian nebula is inferred to have varied roughly as $\Sigma \propto r^{-2.5}$ (Kargel 1987). The surface densities in protoplanetary (and protosatellite) disks appear to commonly follow power laws, with slopes much steeper than the standard MMSN slope of -1.5.

5.2. *Disk Evolution*

The steepness of our inferred surface density, with slope -2.168, is not consistent with a steady state profile in an *accretion* disk, where mass is moving inward. Relaxation of the steady state assumption by using the self-similar evolving disk profiles of Lynden-Bell & Pringle (1974) leads to an instantaneous fit but

tends to evolve too rapidly before and after this match to be consistent with other constraints that apply at other times. The surface density we infer from the augmented masses of planets is a measure of the local density of planetesimals, at the time that they formed and decoupled from the gas. As planetesimals in the 5–10 AU region must have formed more rapidly than planetesimals in the 15–30 AU region, this tends to argue that the surface density we have derived was in place early on and was maintained during planetesimal formation, and to argue against profiles that are rapidly evolving while planetesimals are forming. Other problems with the timing of constraints in the evolving models are that the density in the chondrule-forming regions is too low by 2 Myr to be consistent with chondrule formation in nebular shocks, and the density of gas in the 10–15 AU region falls off very rapidly with time, increasing the time needed to form Uranus's core well beyond a reasonable lifetime of the disk.

These problems do not exist in the steady state model we have described here. In our model, photoevaporation by nearby external stars imposes an outer boundary condition on the disk (at r_d) and is the driver for *outward* mass flow through the outer solar nebula, leading to a surface density profile $\Sigma(r) = (-\dot{M})/(3\pi\nu) \times [(r_d/r)^{1/2} - 1]$. This solution has many commonalities with viscously spreading circumstellar decretion disks (Lee et al. 1991). We have shown that this solution, with two parameters, fits the surface density of the solar nebula exceptionally well. For reasonable parameters, the gas densities in the 10–15 AU region can be maintained for 10 Myr in steady state. One necessary parameter is that $\alpha \approx 4 \times 10^{-4}$; as it happens, this is the value of α inferred from the size sorting of chondrules in the solar nebula. The associated mass flux through the outer solar nebula is then $\dot{M} = -5 \times 10^{-9} (f_p/0.5)\ M_\odot\ \mathrm{yr}^{-1}$, which implies an outward bulk velocity of gas $v_r = -\dot{M}/(2\pi r\Sigma) \approx 1.4\ \mathrm{cm\ s}^{-1}$ that is fairly uniform with radius. At these outward flow speeds, dust entrained in the gas will be swept outward from 2 to 15 AU, where comets form, in <5 Myr. This does not include turbulent diffusion that will be associated with the outward flow of mass, which will spread material farther out even faster (Cuzzi et al. 2005). This result, that gas from the inner solar nebula, as well as any small solids entrained in it, will flow from the inner solar nebula to the comet-forming region beyond about 15 AU, within the disk's lifetime, certainly will be central to resolving the mystery of how high-temperature minerals (e.g., a CAI-like grain) were discovered in comet 81P/Wild 2 by the *Stardust* mission (Zolensky et al. 2006).

5.3. *Planet Formation*

The starting locations of the planets inferred from the Nice model, as well as the consequent surface density of the nebula they imply, are highly favorable for the growth of planets. Previous estimates of the timescale to form Uranus and Neptune, in their current locations using MMSN surface densities, were longer than the age of the solar system, eliminating the possibility of the formation in situ (Lissauer & Stewart 1993). The surface density profile we infer for the solar nebula applies early on, when planetesimals formed; depending on how the disk evolved after that, formation of Uranus could take ≈18 Myr (viscously spreading disk) or, in our steady state photoevaporated disk, as little as 10 Myr. Our disk model explains, for the first time, how *all* the giant planets could have formed within the lifetime of the disk, thereby enabling Uranus and Neptune to accrete H/He envelopes.

Planet formation is so robust that the intriguing possibility exists that another large planet could have formed beyond Uranus, in the planetesimal disk itself. Given the typical spacings between the planets in the outer solar system, we presume that this planet would have formed at about 17 AU. From Figure 4 we see that it reasonably could have grown to about 2 $M_\oplus$ in size. If such a planet did form, we speculate that it was ejected during the orbital chaos that followed Jupiter and Saturn's 2:1 MMR crossing. The size of this planet is smaller than the uncertainty in the initial mass of the planetesimal disk, so it is not clear how its one-time presence in the solar system could be detected. One wonders whether Earth mass ice planets ejected from other solar systems could be detected observationally.

The magnitude and slope of the surface density of planetesimals will have a bearing on the number of planets that form, as well as their relative sizes. Simulations of Jupiter's growth typically invoke surface densities of planetesimals in its vicinity ≈10 g cm^{-2} (Pollack et al. 1996; Chambers 2006). Notably, planets much smaller than Jupiter tend to form (and take longer to do so) when the surface density is as low as that implied by standard MMSN models. Also, it has been recognized for some time that the cores and metal contents of the giant planets are very similar, despite Jupiter being 20 times more massive than Uranus. This implies that the isolation masses of the planets' cores were similar (Pollack et al. 1996). In fact, Pollack et al. (1996) suggested on this basis that the surface density in the solar nebula varied as r^{-2} because the isolation masses scale as $(\Sigma r^2)^{3/2}$. We find that this conclusion is largely borne out, as the slope of our surface density is near −2. We have shown in Figure 4 that the final metal contents of each giant planet are consistent with it consuming all planetesimals in its feeding zone. These final masses do decrease with increasing heliocentric distance, although slightly more rapidly than expected, largely because the planets' feeding zones tend not to be the same number of Hill radii across. For surface densities $\Sigma = \Sigma_0(r/r_0)^{-p}$, Kokubo & Ida (2002) found that, generally, only large values of Σ_0 lead to a small number of planets, and only if $p > 2$ do the planet sizes decrease with distance from the Sun, as they do in our solar system.

This raises the intriguing possibility that solar system architecture may depend on the star formation environment. Stars that did not form in the face of photoevaporation are more likely to viscously spread and have lower densities. We speculate that planet formation would be frustrated beyond about 10 AU in such disks. If the surface densities were shallower in such disks, there would possibly be a larger number of smaller planets, growing in size with distance from the star (see Fig. 9 of Kokubo & Ida 2002).

5.4. *Validity of a Minimum-Mass Solar Nebula*

In this paper we have argued that the very concept of a minimum-mass solar nebula is valid only under certain conditions. First, the concept of a single surface density profile relevant to the solar nebula is valid only in the limit that the surface density is maintained for periods long compared to nebular evolution. In this paper we have demonstrated that in contrast to a viscously spreading disk, high gas densities can be maintained for many millions of years, up to 10 Myr in the 10–15 AU region. Second, calculation of this surface density profile relies on the giant planets exhausting their feeding zones of planetesimals. Here we have shown that, using our derived surface density profile, the metal contents M_Z of the giant planets are consistent with all of them consuming all of the available planetesimals in their feeding zones. If the fraction of all solids that grew to planetesimal size is independent of radius, as simulations seem to indicate (Weidenschilling 1997),

then the surface density of the solar nebula gas safely may be estimated by assuming an augmented mass $M_Z f_p^{-1}$(gas/solids) for each planet's feeding zone, then dividing by the area of the feeding zone. It is certainly not *required* that the solar nebula could be described using an α viscosity and that it conformed to a steady state profile because its outer boundary was photoevaporated; but within the context of these assumptions, we find that growth of all of the giant planets, including Uranus and Neptune, to their isolation masses is ensured. This makes our model of the protoplanetary disk and the growth of planets within it the *first* self-consistent model of the solar nebula. Finally, the fact that the giant planets achieved their isolation masses means that our inferred surface density profile is not just a *minimum-mass* profile but represents the *actual* density profile of our solar nebula, within its first few Myr of evolution.

The author would like to thank Jeff Hester and Sean Raymond for discussions that contributed to the writing of this paper and Aaron Boley for a critical review of the paper. The author thanks an anonymous referee for comments that led to significant improvements in this paper. The author thanks Hal Levison and Stu Weidenschilling for helpful critical reviews of an earlier draft of this paper. This work was partially supported by grant NNG06GI65G through NASA's Origins of Solar Systems program.

REFERENCES

Adams, F. C., Hollenbach, D., Laughlin, G., & Gorti, U. 2004, ApJ, 611, 360
Alfvén, H., & Arrhenius, G. 1970, Ap&SS, 8, 338
Andrews, S. M., & Williams, J. P. 2005, ApJ, 631, 1134
Asphaug, E., & Benz, W. 1994, Nature, 370, 120
Beckwith, S. V. W., Sargent, A. I., Chini, R. S., & Guesten, R. 1990, AJ, 99, 924
Bodenheimer, P., & Pollack, J. B. 1986, Icarus, 67, 391
Boley, A. C., Durisen, R. H., Nordlund, A., & Lord, J. 2007, ApJ, 665, 1254
Boss, A. P. 2000, ApJ, 536, L101
Chambers, J. E. 2006, ApJ, 652, L133
Chiang, E. I., & Brown, M. E. 1999, AJ, 118, 1411
Chiang, E. I., & Goldreich, P. 1997, ApJ, 490, 368
Ciesla, F. J., & Hood, L. L. 2002, Icarus, 158, 281
Cuzzi, J. N., Ciesla, F. J., Petaev, M. I., Krot, A. N., Scott, E. R. D., & Weidenschilling, S. J. 2005, in ASP Conf. Ser. 341, Chondrites and the Protoplanetary Disk, ed. A. N. Krot, E. R. D. Scott, & B. Reipurth (San Francisco: ASP), 732
Cuzzi, J. N., Hogan, R. C., Paque, J. M., & Dobrovolskis, A. R. 2001, ApJ, 546, 496
Cuzzi, J. N., & Weidenschilling, S. J. 2006, in Meteorites and the Early Solar System II, ed. D. S. Lauretta & H. Y. McSween, Jr. (Tucson: Univ. Arizona Press), 353
Davis, S. S. 2003, ApJ, 592, 1193
———. 2005, ApJ, 627, L153
Desch, S. J., & Connolly, H. C., Jr. 2002, Meteoritics Planet. Sci., 37, 183
Dubrulle, B. 1993, Icarus, 106, 59
Edgeworth, K. E. 1949, MNRAS, 109, 600
Eisner, J. A., & Carpenter, J. M. 2006, ApJ, 641, 1162
Fernandez, J. A., & Ip, W.-H. 1984, Icarus, 58, 109
Gammie, C. F. 2001, ApJ, 553, 174
Gomes, R., Levison, H. F., Tsiganis, K., & Morbidelli, A. 2005, Nature, 435, 466
Gomes, R. S., Morbidelli, A., & Levison, H. F. 2004, Icarus, 170, 492
Guillot, T. 2005, Annu. Rev. Earth Planet. Sci., 33, 493
Guillot, T., Stevenson, D. J., Hubbard, W. B., & Saumon, D. 2004, in Jupiter: The Planet, Satellites and Magnetosphere, ed. F. Bagenal, T. E. Dowling, & W. B. McKinnon (Cambridge: Cambridge Univ. Press), 35
Haisch, K. E., Jr., Lada, E. A., & Lada, C. J. 2001, ApJ, 553, L153
Hartmann, L., Calvet, N., Gullbring, E., & D'Alessio, P. 1998, ApJ, 495, 385
Hayashi, C. 1981, Prog. Theor. Phys. Suppl., 70, 35
Hayashi, C., Nakazawa, K., & Nakagawa, Y. 1985, in Protostars and Planets II, ed. D. C. Black & M. S. Mathews (Tucson: Univ. Arizona Press), 1100
Hollenbach, D., & Adams, F. C. 2004, in ASP Conf. Ser. 324, Debris Disks and the Formation of Planets, ed. L. Caroff et al. (San Francisco: ASP), 168
Hollenbach, D. J., Yorke, H. W., & Johnstone, D. 2000, in Protostars and Planets IV, ed. V. Mannings, A. P. Boss, & S. S. Russell (Tucson: Univ. Arizona Press), 401
Hueso, R., & Guillot, T. 2005, A&A, 442, 703
Ida, S., & Makino, J. 1993, Icarus, 106, 210
Ida, S., & Nakazawa, K. 1989, A&A, 224, 303
Inaba, S., & Ikoma, M. 2003, A&A, 410, 711
Kargel, J. S. 1987, Lunar and Planetary Institute Conference Abstracts, 18, 477
Kenyon, S. J., & Hartmann, L. 1995, ApJS, 101, 117
Kenyon, S. J., & Luu, J. X. 1999, ApJ, 526, 465
Kokubo, E., & Ida, S. 2002, ApJ, 581, 666
Königl, A. 1991, ApJ, 370, L39
Kuchner, M. J. 2004, ApJ, 612, 1147
Kuiper, G. P. 1956, J. R. Astron. Soc. Canada, 50, 158
Lee, U., Osaki, Y., & Saio, H. 1991, MNRAS, 250, 432
Levison, H. F., Morbidelli, A., Gomes, R., & Backman, D. 2007, in Protostars and Planets V, ed. B. Reipurth, D. Jewitt, & K. Keil (Tucson: Univ. Arizona Press), 669
Lide, D. R. 1992, CRC Handbook of Physics and Chemistry (London: CRC Press)
Lissauer, J. J., & Stewart, G. R. 1993, in Protostars and Planets III, ed. E. H. Levy & J. I. Lunine (Tucson: Univ. Arizona Press), 1061
Lodders, K. 2003, ApJ, 591, 1220
Lunine, J. I., Yung, Y. L., & Lorenz, R. D. 1999, Planet. Space Sci., 47, 1291
Lynden-Bell, D., & Pringle, J. E. 1974, MNRAS, 168, 603
Malhotra, R. 1993, Nature, 365, 819
Mizuno, H. 1980, Prog. Theor. Phys., 64, 544
Mizuno, H., Nakazawa, K., & Hayashi, C. 1978, Prog. Theor. Phys., 60, 699
Morbidelli, A., Levison, H. F., & Gomes, R. 2007, preprint (astro-ph/0703558)
Morbidelli, A., Levison, H. F., Tsiganis, K., & Gomes, R. 2005, Nature, 435, 462
Niemann, H. B., et al. 1998, J. Geophys. Res., 103, 22831
Osterloh, M., & Beckwith, S. V. W. 1995, ApJ, 439, 288
Podolak, M., Podolak, J. I., & Marley, M. S. 2000, Planet. Space Sci., 48, 143
Pollack, J. B., Hubickyj, O., Bodenheimer, P., Lissauer, J. J., Podolak, M., & Greenzweig, Y. 1996, Icarus, 124, 62
Pringle, J. E. 1981, ARA&A, 19, 137
Raymond, S. N., Quinn, T., & Lunine, J. I. 2005, ApJ, 632, 670
Safronov, V. S. 1967, Soviet Astron., 10, 650
Saumon, D., & Guillot, T. 2004, ApJ, 609, 1170
Shakura, N. I., & Sunyaev, R. A. 1973, A&A, 24, 337
Stone, J. M., Gammie, C. F., Balbus, S. A., & Hawley, J. F. 2000, in Protostars and Planets IV, ed. V. Mannings, A. P. Boss, & S. S. Russell (Tucson: Univ. Arizona Press), 589
Takeuchi, T., & Lin, D. N. C. 2002, ApJ, 581, 1344
Tera, F., Papanastassiou, D. A., & Wasserburg, G. J. 1974, Earth Planet. Sci. Lett., 22, 1
Trujillo, C. A., & Brown, M. E. 2001, ApJ, 554, L95
Tsiganis, K., Gomes, R., Morbidelli, A., & Levison, H. F. 2005, Nature, 435, 459
Wadhwa, M., Amelin, Y., Davis, A. M., Lugmair, G. W., Meyer, B., Gounelle, M., & Desch, S. J. 2007, in Protostars and Planets V, ed. B. Reipurth, D. Jewitt, & K. Keil (Tucson: Univ. Arizona Press), 835
Weidenschilling, S. J. 1977a, Ap&SS, 51, 153 (W77)
———. 1977b, MNRAS, 180, 57
———. 1997, Icarus, 127, 290
———. 2000, Space Sci. Rev., 92, 295
Weidenschilling, S. J., & Cuzzi, J. N. 1993, in Protostars and Planets III, ed. E. H. Levy & J. I. Lunine (Tucson: Univ. Arizona Press), 1031
Zolensky, M. E., et al. 2006, Science, 314, 1735